15. Shinmura,K. *et al.* (2004) Inactivating mutations of the human base excision repair gene *NEIL1* in gastric cancer. *Carcinogenesis*, **25**, 2311–2317.
16. Kobayashi,K. *et al.* (2008) Frequent splicing aberration of the base excision repair gene hMYH in human gastric cancer. *Anticancer Res.*, **28**, 215–221.
17. Tsukino,H. *et al.* (2004) *hOGG1* Ser326Cys polymorphism, interaction with environmental exposures, and gastric cancer risk in Japanese populations. *Cancer Sci.*, **95**, 977–983.
18. Takezaki,T. *et al.* (2002) *hOGG1* Ser(326)Cys polymorphism and modification by environmental factors of stomach cancer risk in Chinese. *Int. J. Cancer*, **99**, 624–627.
19. Cheadle,J.P. *et al.* (2007) *MUTYH*-associated polyposis—from defect in base excision repair to clinical genetic testing. *DNA Repair (Amst.)*, **6**, 274–279.
20. Shinmura,K. *et al.* (2008) Induction of centrosome amplification and chromosome instability in *p53*-deficient lung cancer cells exposed to benzo[a]pyrene diol epoxide (B[a]PDE). *J. Pathol.*, **216**, 365–374.
21. Goto,M. *et al.* (2008) *OGG1*, *MYH* and *MTH1* gene variants identified in gastric cancer patients exhibiting both 8-hydroxy-2′-deoxyguanosine accumulation and low inflammatory cell infiltration in their gastric mucosa. *J. Genet.*, **87**, 181–186.
22. Hara,M. *et al.* (2003) Cruciferous vegetables, mushrooms, and gastrointestinal cancer risks in a multicenter, hospital-based case-control study in Japan. *Nutr. Cancer*, **46**, 138–147.
23. Kaneda,A. *et al.* (2002) Identification of silencing of nine genes in human gastric cancers. *Cancer Res.*, **62**, 6645–6650.
24. Esteller,M. (2008) Epigenetics in cancer. *N. Engl. J. Med.*, **358**, 1148–1159.
25. Koketsu,S. *et al.* (2004) Expression of DNA repair protein: MYH, NTH1, and MTH1 in colorectal cancer. *Hepatogastroenterology*, **51**, 638–642.
26. Ikeda,S. *et al.* (2002) Differential intracellular localization of the human and mouse endonuclease III homologs and analysis of the sorting signals. *DNA Repair (Amst.)*, **1**, 847–854.
27. Cathcart,R. *et al.* (1984) Thymine glycol and thymidine glycol in human and rat urine: a possible assay for oxidative DNA damage. *Proc. Natl Acad. Sci. USA*, **81**, 5633–5637.
28. Adelman,R. *et al.* (1988) Oxidative damage to DNA: relation to species metabolic rate and life span. *Proc. Natl Acad. Sci. USA*, **85**, 2706–2708.
29. Katafuchi,A. *et al.* (2004) Differential specificity of human and *Escherichia coli* endonuclease III and VIII homologues for oxidative base lesions. *J. Biol. Chem.*, **279**, 14464–14471.
30. Basu,A.K. *et al.* (1989) Genetic effects of thymine glycol: site-specific mutagenesis and molecular modeling studies. *Proc. Natl Acad. Sci. USA*, **86**, 7677–7681.
31. Feig,D.I. *et al.* (1994) Reverse chemical mutagenesis: identification of the mutagenic lesions resulting from reactive oxygen species-mediated damage to DNA. *Proc. Natl Acad. Sci. USA*, **91**, 6609–6613.
32. Kamiya,H. *et al.* (2002) Induction of T —> G and T —> A transversions by 5-formyluracil in mammalian cells. *Mutat. Res.*, **513**, 213–222.
33. Kalam,M.A. *et al.* (2006) Genetic effects of oxidative DNA damages: comparative mutagenesis of the imidazole ring-opened formamidopyrimidines (Fapy lesions) and 8-oxo-purines in simian kidney cells. *Nucleic Acids Res.*, **34**, 2305–2315.
34. Radak,Z. *et al.* (2005) Lung cancer in smoking patients inversely alters the activity of hOGG1 and hNTH1. *Cancer Lett.*, **219**, 191–195.
35. Mrkonjic,M. *et al.* (2007) MSH2 118T>C and MSH6 159C>T promoter polymorphisms and the risk of colorectal cancer. *Carcinogenesis*, **28**, 2575–2580.
36. Raptis,S. *et al.* (2007) MLH1 -93G>A promoter polymorphism and the risk of microsatellite-unstable colorectal cancer. *J. Natl Cancer Inst.*, **99**, 463–474.
37. Hu,Z. *et al.* (2005) A promoter polymorphism (-77T>C) of DNA repair gene XRCC1 is associated with risk of lung cancer in relation to tobacco smoking. *Pharmacogenet. Genomics*, **15**, 457–463.
38. Yoo,D.G. *et al.* (2008) Alteration of APE1/ref-1 expression in non-small cell lung cancer: the implications of impaired extracellular superoxide dismutase and catalase antioxidant systems. *Lung Cancer*, **60**, 277–284.

Received January 26, 2009; revised April 6, 2009; accepted April 28, 2009

The American Journal of Pathology, Vol. 175, No. 2, August 2009

DOI: 10.2353/ajpath.2009.080489

Tumorigenesis and Neoplastic Progression

Down-Regulation of DUSP6 Expression in Lung Cancer

Its Mechanism and Potential Role in Carcinogenesis

Koji Okudela,* Takuya Yazawa,* Tetsukan Woo,[†‡] Masashi Sakaeda,* Jun Ishii,* Hideaki Mitsui,* Hiroaki Shimoyamada,* Hanako Sato,*[§] Michihiko Tajiri,[‡] Nobuo Ogawa,[‡] Munetaka Masuda,[†] Takashi Takahashi,[¶] Haruhiko Sugimura,[‖] and Hitoshi Kitamura*

From the Departments of Pathology and Surgery,[†] Yokohama City University Graduate School of Medicine, Yokohama; the Division of General Thoracic Surgery,[‡] Kanagawa Cardiovascular and Respiratory Disease Center Hospital, Yokohama; the Department of Anatomy,[§] St. Marianna University School of Medicine, Kawasaki; the Division of Molecular Carcinogenesis,[¶] Center for Neurological Disease and Cancer, Nagoya University Graduate School of Medicine, Nagoya; and the Department of Pathology,[‖] Hamamatsu Medical University, School of Medicine, Hamamatsu, Japan*

Our preliminary studies revealed that oncogenic KRAS (KRAS/V12) dramatically suppressed the growth of immortalized airway epithelial cells (NHBE-T, with viral antigen-inactivated p53 and RB proteins). This process appeared to be a novel event, different from the so-called premature senescence that is induced by either p53 or RB, suggesting the existence of a novel tumor suppressor that functions downstream of oncogenic KRAS. After a comprehensive search for genes whose expression levels were modulated by KRAS/V12, we focused on DUSP6, a pivotal negative feedback regulator of the RAS-ERK pathway. A dominant-negative DUSP6 mutant, however, failed to rescue KRAS/V12-induced growth suppression, but conferred a stronger anchorage-independent growth activity to the surviving subpopulation of cells generated from KRAS/V12-transduced NHBE-T. DUSP6 expression levels were found to be weaker in most lung cancer cell lines than in NHBE-T, and DUSP6 restoration suppressed cellular growth. In primary lung cancers, DUSP6 expression levels decreased as both growth activity and histological grade of the tumor increased. Loss of heterozygosity of the *DUSP6* locus was found in 17.7% of cases and was associated with reduced expression levels. These results suggest that DUSP6 is a growth suppressor whose inactivation could promote the progression of lung cancer. We have here identified an important factor involved in carcinogenesis through a comprehensive search for downstream targets of oncogenic KRAS. ***(Am J Pathol 2009, 175:867–881; DOI: 10.2353/ajpath.2009.080489)***

Oncogenic mutations of *KRAS* occur very early in carcinogenesis of the lung and affect even premalignant lesions.[1,2] It is therefore likely that additional genetic and/or epigenetic alterations are necessary for lung neoplasms to develop into advanced form of cancers. The inactivation of putative tumor suppressors, p53 and p16INK4A/RB protein, and activation of telomerase, are generally accepted as crucial to the promotion carcinogenesis.[1,3] A recent study, however, reported that these alterations are not enough to provide primary bronchial epithelial cells with a fully malignant phenotype *in vitro*,[4] and suggested further alterations would be necessary for the progression of lung cancer.

DUSP6, dual-specificity phosphatase 6, is a putative negative feedback regulator for the RAS-ERK pathway, playing physiologically important role(s) in the maintenance of cellular homeostasis in response to growth factors.[5–11] Disruption of this feedback loop could therefore result in neoplastic, and even malignant, transformation by providing cells with enhanced growth activity. Actually, a series of previous studies reported the involvement of DUSP6 down-regulation caused by the hypermethyl-

Supported by the Japanese Ministry of Education, Culture, Sports and Science (Tokyo, Japan), by the Smoking Research Foundation, and by a grant from the Yokohama Medical Facility (Yokohama, Japan).

Accepted for publication May 13, 2009.

Supplemental material for this article can be found on *http://ajp.amjpathol.org*.

Address reprint requests to Hitoshi Kitamura, Department of Pathology, Yokohama City University Graduate School of Medicine, 3-9 Fukuura, Kanazawa-Ku, 236-0004 Yokohama, Japan. E-mail: pathola@med.yokohama-cu.ac.jp.

ation of its promoter in the progression of pancreatic cancers.[12–16] To our knowledge, however, there have been only a few reports investigating the significance of DUSP6 in other types of cancers including lung cancers.[4,17]

Our preliminary study revealed that oncogenic KRAS (KRAS/V12) dramatically suppressed growth of immortalized airway epithelial cells whose p53 and RB proteins were inactivated by viral antigens. This seemed a novel event different from so-called premature senescence that is induced by p53 or RB pathway,[3] and suggested there might exist novel tumor suppressors downstream of oncogenic KRAS. Thus, we have been interested in identifying such suppressors. Also, our recent study demonstrated that insulin-like growth factor-binding proteins 2 and 4, downstream targets of oncogenic KRAS, suppress the growth of cancer cells in a negative-feedback manner and that disruption of this feedback loop, through their promoter's hypermethylation, is possibly involved in the progression of lung cancers.[18] It is worth noting that growth suppressors lie hidden downstream of the signal transduction pathway of an oncogene. Thus, we were prompted to search for downstream targets of oncogenic KRAS comprehensively, to further identify potential growth suppressors. Among genes whose expression was modulated by oncogenic KRAS, this study has focused on DUSP6, and elucidated its role in the KRAS-induced growth suppression and in carcinogenesis of the lung.

Materials and Methods

Cell Culture

An immortalized human airway epithelial cell line (16HBE14o, Simian virus 40-transformed human bronchial epithelial cells), described by Cozens et al,[19] was kindly provided by Grunert DC (California Pacific Medical Center Research Institute) via Kaneko T (Yokohama City University School of Medicine). A subclone of 16HBE14o cells, described as NHBE-T in this paper, was used for experiments. Immortalized airway epithelial cell lines (HPL1D and HPL1A, Simian virus 40-transformed human small airway epithelial cells) were established by Masuda et al.[20] Human lung cancer cell lines (A549, H358, and H1299) and the human embryonic kidney cell line (HEK293T) were purchased from American Type Culture Collection (ATCC, Manassas, VA). Human lung cancer cell lines, LC2/ad, Lu134A, Lu140, and PC9, were obtained form Riken Cell Bank (Tsukuba, Japan), and Immuno-Biological Laboratories Co. (Gunma, Japan), respectively. Human lung cancer cell lines, TKB1, TKB2, TKB4, TKB5, TKB6, TKB7, TKB8, TKB12, TKB15, TKB16, TKB17, and TKB20 were kindly provided by Kamma H (Kyorin University School of Medicine, Tokyo Japan). The cells were cultured and grown in DMEM (Sigma Aldrich, St. Louis, MO) (NHBE-T, HPL1D, HPL1A, A549, H358, PC9, LC2/ad, TKB1, TKB2, TKB4, TKB5, TKB6, TKB7, TKB8, TKB2, and H1299) or RPMI1640 medium (Sigma) (Lu130, Lu134A, Lu140, HEK293T, TKB12, TKB15, TKB16, and TKB17) supplemented with 10% heat-inactivated fetal bovine serum (Sigma), 100 units/ml of penicillin (Sigma), and 100 μg/ml of streptomycin (Sigma).

Cell Growth Assays

Cells (2.5×10^5) were seeded onto a 10-cm culture dish (Iwaki, Tokyo, Japan), and grown to a semiconfluent state for 5 to 7 days. The cells were counted, and 2.5×10^5 cells were seeded again onto a 10-cm dish. Several passages were repeated in the same manner. The sum of population doublings (PDLs) at each point, was calculated by the formula $\Sigma PDL_n = \log_2 (count_n/2.5 \times 10^5) + \Sigma PDL_{n-1}$.

Colony Formation Assays

Cells (1.0×10^4 or 5.0×10^4) were seeded onto a 10-cm culture dish (Iwaki), and grown for optimal period (8 to 14 days). The cells were fixed with methanol and Giemsa-stained, and colonies visible in scanned photographs were counted.

Soft Agar Colony Formation Assays

Cells (1.25×10^4) were grown in 1 ml of DMEM-based 0.3% agar (agar noble; Becton Dickinson, Sparks, MD) containing 10% fetal bovine serum in a 3.5-cm culture dish (Iwaki) for 5 weeks. The agar was fixed with a buffered 4% paraformaldehyde solution, and colonies visible in scanned photographs were counted.

Plasmid Construction

cDNA encoding wild-type KRAS (KRAS/G12) and mutated KRAS (KRAS/V12) were PCR-amplified (PrimeSATR HS DNA polymerase, Takara Bio Inc., Kyoto, Japan) with primers having BamH1 restriction sites (forward (F), 5′-CTCCGC*GGATCC*AAGCTTGCTGAAA-3′ and reverse (R), 5′-AGGGGC*GGATCC*TCATTACATAA-3′; the BamH1 restriction sites are in italics). Plasmid vectors, pcDNA3.1-KRAS/G12 and -KRAS/V12 described previously,[2] were used as templates. The amplified fragments were digested with BamH1 (Takara), and inserted into pQCXIH retroviral provirus vectors (BD Clontech, Palo Alto, CA). cDNA encoding DUSP6 variant 2 (Gene Bank Accession # BC003143) was PCR-amplified (PrimeSATR HS DNA polymerase, Takara) with primers (F, 5′-GCTCGACCCCCATGATAGATACG-3′ and R, 5′-CATTCCAGCAAGGAGGGATGTGG-3′), using cDNA reverse-transcribed (SuperScript III, Invitrogen, Carlsbad, CA) from NHBE-T-derived polyadenylated RNA as a template. After the adenylation of 3′ terminals with TaqDNA polymerase (Takara), the amplified fragment was subcloned into the pT7Blue vector (Novagen, Darmstadt, Germany). The DUSP6 cDNA was PCR-amplified (PrimeSATR HS DNA polymerase, Takara) again using pT7Blue/DUSP6 as a template with mismatch primers having BamH1 restriction sites (F, 5′-GATTGC*GGATCC*GGCATGATAGAT-

ACGCTCAG-3′ and R, 5′-TCCAGCAAGGAG*GGATC*-*C*GGGGTCTTTCAC-3′; BamH1 restriction sites are in italics). After digestion with BamH1 (Takara), the fragment was inserted into pQCXIP (BD Clontech). A dominant negative mutant of DUSP6 that had lost its phosphatase activity (DUSP6/C293S: Cysteine at position-293 was converted to Serine)[8] was generated using a site-directed mutagenesis kit (Stratagene, La Jolla, CA) with mismatch primers (5′-GTCTTGGTACAT*A*GCTTGGCTG-GCATTAG-3′ and 5′-CTAATGCCAGCCAAGC*T*ATGTAC-CAAGAC-3′: mismatch bases are in italics). A retroviral provirus vector (psiDKI, Takara) expressing siRNA targeting two positions of DUSP6 mRNA (5′-CCAACCA-GAATGTATACCA-3′ [+1103 to +1121] and 5′-GAACT-GTGGTGTCTTGGTA-3′ [+855 to +873]) and the same sized siRNA with scramble sequences were constructed according to the manufacturer's instruction (Takara). Candidate promoter regions of −1539 to +24, −1030 to + 24, and −539 to + 24 at the DUSP6 gene locus (NC_000012) (position of the first base (A) of the start codon [ATG] was determined as + 1), were PCR-amplified (PrimeSATR HS DNA polymerase, Takara) with primer sets, F-1539, 5′-GGTCTTGCGG-GAGGACTT-3′ and *r* + 24, 5′-CACGGGTCTGAGC-TATCT-3′; F-1030, 5′-CAAACAGACCTGGGC-CTTTA-3′ and *r* + 24, 5′-CACGGGTCTGAGCTATCT-3′; F-511, 5′-GAGACGCTCGCTGTTTGTATC-3′ and *r* + 24, 5′-CACGGGTCTGAGCTATCT-3′, using genomic DNA extracted from non-tumor parts of surgically resected lung as a template. After adenylation of the 3′ terminals with TaqDNA polymerase (Takara), the products were subcloned into pT7Blue (Novagen). They were then cut out with HindIII (Takara) and KpnI (Takara), and inserted into pGL4.1 (Promega, Madison, WI). The accuracy of all of the constructs was verified by DNA sequencing (Dye-deoxy DNA sequencing kit, Amersham Life Science, Piscataway, NJ).

Retroviral-Mediated Gene Transfer

The pQCXIP(H)-based expression vectors and pDKsi based-knockdown vectors designed as described above and the pCL10A1 retrovirus packaging vector (Imgenex, San Diego, CA) were cotransfected into HEK293T cells with Lipofectamine 2000 reagent (Invitrogen). At 24 hours after the transfection, conditioned medium was recovered as a viral solution. Desired genes were introduced by incubating cells with the viral solution containing 10 μg/ml of polybren (Sigma) for 24 hours. Cells stably expressing desired genes were selected with 1.0 μg/ml of puromycin (or 500 μg/ml hygromycin B or 1000 μg/ml of neomycin [G418]) (Invitrogen) for 3 days. The pooled clones were used for biological analyses and expression profiling.

Expression Profiling

Gene expression in the empty vector-, KRAS/G12-, and KRAS/V12-transduced NHBE-T cells was comprehensively evaluated with an U133A human gene chip microarray (Affymetrix, San Diego, CA) according to the manufacturer's recommendations. In brief, total RNA was extracted from the cells immediately after completion of the selection (5 days post-transduction), and was reverse transcribed with Super Script II reverse transcriptase (Invitrogen). Complementary RNA was transcribed *in vitro* using T7 RNA polymerase (Invitrogen) and concomitantly labeled with a fluorescent dye. The labeled complementary RNA was fragmented by acetic acid treatment, and hybridized to the cDNA array. The hybridized signals were scanned with a Gene Chip Scanner 3000 (Affymetrix), and the signal values of each probe were globally normalized according to manufacture's recommendation. It was checked that differences in signal values of house keeping genes including β-actin (ACTB) and glyceraldehyde-3-phosphate dehydrogenase among the transfectants were no more than 1.5-fold. Probes showing an absence call were excluded. Then, a hierarchical clustering analysis (Ward's Method) was performed with computer software (GeneSpring, Agilent technology, Palo Alto, CA). Probes (= genes) whose signal values were elevated or reduced more than fivefold by the KRAS/V12 transduction in comparison with both the empty vector transduction and the KRAS/G12 transduction were extracted by using GeneSpring (Agilent Technology).

Quantitative Reverse Transcription-PCR

First-strand cDNA was synthesized from total RNA using the SuperScript First-Strand Synthesis System according to the protocols of the manufacturer (Invitrogen). The cDNA generated was used as a template in real-time PCR with SYBR Premix EXTaq (Takara) and run on a Thermal Cycler DICE real-time PCR system (Takara). The primer set used for the detection of DUSP6 was F, 5′-AACAGGGTTCCAGCACAGCAG-3′; R, 5′-GGCCA-GACACATTCCAGCAA-3′. That for ACTB was F, 5′-TG-GCACCCAGCACAATGAA-3′; R, 5′-CTAAGTCATAGTC-CGCCTAGAAGCA-3′. The means and standard deviations of the copy number of DUSP6 normalized to the value for ACTB mRNA were statistically obtained from triplicate reactions.

Western Blotting

The cells grown to subconfluence were solved with extraction buffer, as described elsewhere.[2] After centrifugation, supernatants were recovered as protein extracts. The extracts were mixed with equal volumes of 2×SDS buffer, and then boiled. The samples were subjected to SDS-polyacrylamide gel electrophoresis, and transferred onto polyvinylidene difluoride membranes (Amersham). The membranes were incubated with nonfat dry milk in 0.01 M/L Tris-buffered saline containing 0.1% Tween-20 to block non-immunospecific protein binding, and then with 0.1 μg/ml of primary antibody against either KRAS (Santa Cruz, Santa Cruz, CA), DUSP6 (Abnova), ERK (Cell Signaling Technology, Beverly, MA), phosphorylated ERK (Cell Signaling Technology), or β-actin (Sigma). After

washing with 0.01 M/L Tris-buffered saline containing 0.1% Tween-20, the membranes were incubated with animal-matched horseradish peroxidase-conjugated secondary antibodies (Amersham). Immunoreactivity was visualized with the enhanced chemiluminescence system (ECL, Amersham).

Treatment with 5-Azacytidine and Trichostatin A

Cells were treated either with 10 μmol/L of 5-azacytidine (AZA, Sigma) for 72 hours by exchanging the medium everyday or with 300 ng/ml of trichostatin A (TSA, Wako, Osaka, Japan) for 24 hours. In addition, cells were treated also with AZA for 48 hours and then with a combination of AZA and TSA for an additional 24 hours.

Bisulfate Conversion-Based DNA Sequencing

Genomic DNA was extracted from cultured cells as described previously,[2] and subjected to bisulfate conversion treatment using a MethylEasy DNA bisulfate modification kit (Human Genetic Signatures, Macquarie Park, Australia) according to the manufacturer's instructions. The region from −960 to −266 of the DUSP6 gene, including the promoter locus, was PCR-amplified (TaqHS DNA polymerase, Takara) with three sets of primers (F1, 5′-GAGTTGGGTTTTTAAAGTGGTAAATA-3′ and R1, 5′-CAAAACACATAAACCAAAACACTTC-3′; F2, 5′-GAAATATGAGATAATTGAAGTGTTTTGG-3′ and R2, 5′-CAACTCCTCAATAAATACAAACAAC-3′; F3, 5′-TGTTTGTATTTATTGAGGAGTTGTTT-3′ and R3, 5′-CTACCCAAATAATTTTTATTCCTCC-3′), and subcloned into pT7Blue (Novagen). Eight clones were randomly chosen, and nucleotide conversions at CpG sites were searched for, by DNA sequencing (Dye-deoxy DNA sequencing kit, Amersham).

Bisulfate Conversion-Based Methylation-Specific PCR

The region from +544 to +627 in intron 1 of the DUPS6 gene, reported to be highly methylated in pancreatic cancers,[16] was PCR-amplified (TaqHS DNA polymerase, Takara) with primers specific for either methyl (F, 5′-GTAGGGGTCGCGAATCGCGC-3′ and R, 3′-ACCGCCGTAACCCGCAACCG-3′) or un-methyl DNA (F, 5′-GTAGGGGTTGTGAATTGTGT-3′ and R, 5′-AACCACCAATACCCACAACCA-3′)[16] using bisulfate-converted DNA as a template.

Luciferase Reporter Assays

The pGL4.1-based vectors bearing the 5′-untranslated region of the DUSP gene (described in the section Plasmid Construction) and pGL4.7-TK Renilla (Promega, Madison) were co-transfected into NHBE-T cells with Lipofectamine 2000 (Invitrogen). After 24 hours, cells were solved, and luminosity was measured using a Dual Luciferase Reporter Assay system (Promega) on a luminometer (TD-20/20, Turner BioSystems, Sunnyvale, CA). The luminosity derived from each pGL4.1-based vector was corrected with that from pGL4.7-TK Renilla, to normalize the transfection efficiency. Luminosity relative to that of an empty pGL4.1 vector was determined as promoter activity.

Bromodeoxyuridine Pulse Labeling

Cells were incubated in the ordinal medium (DMEM with 10% fetal bovine serum) containing 10 μmol/L of bromodeoxyuridine (BrdU, Sigma) for 45 minutes, thereafter fixed with 4% paraformaldehyde, and then treated with 1N HCl to denature DNA. Incorporated BrdU was visualized by immunocytochemistry with a specific antibody against BrdU (Becton Dickinson, San Jose, CA) using an EnVSION detection system (DakoCytomation, Dako, Ely, UK). A thousand or more cell nuclei were counted, and the percentage of positively labeled cells was determined as a pulse-labeling index.

Flow Cytometry

Cells were harvested by trypsinization, fixed with cold 70% ethanol, and treated with 10 mg/ml of RNase A (Sigma). The cells were suspended in 50 μg/ml of propidium iodide. DNA content was measured with a flow cytometer (Epics Elite; Beckman Coulter, Fullerton, CA).

Primary Lung Cancers

All cases examined were of lung cancer patients who underwent surgical resection at Kanagawa Cardiovascular and Respiratory Disease Center Hospital between 2001 and 2008. Informed consent for research use was obtained from all of the subjects providing materials. One hundred and seventy-two cases (adenocarcinomas [ADC, 107], squamous cell carcinomas [SQC, 51], and large cell carcinomas [LCC, 14]), were examined for KRAS codon 12 mutations by restriction endonuclease-mediated selective PCR[21] as described below. Twenty-two cases (ADC,[18] LCC,[3] and SQC[1]) were found to have a mutated KRAS (12.8%). The cases with *KRAS* mutations and 74 cases of non-small cell lung cancer without a *KRAS* mutation, a total of 96 cases, were used for further analyses. ADCs were classified into histological subtypes according to the criteria of the World Health Organization.[22] If the case involved a mixed type, the major component was described as the subtype in the present study.

REMS-PCR Analysis for Detection of KRAS Codon 12 Mutations

Genomic DNA was extracted from fresh frozen lung cancer tissues or paraffin sections by methods described previously.[2,21] For detection of *KRAS* codon 12 mutations, the RESMS PCR described by Ward et al was partially modified. Briefly, the reaction mixture, a final

volume of 5 μl, containing 0.5 μl of 10 ng/μl DNA solution (1 ng/μl), 0.5 μl of 10×PCR buffer (1×), 0.4 μl of each 2.5 mmol/L dNTP (0.2 mmol/L), 0.04 μl of 50 μmol/L primes (three primer sets described by Ward et al, each 0.4 μmol/L), 0.025 μl of TaqHS DNA polymerase (Takara), 0.4 μl of BstN1 (New England BioLabs, Northbrook, IL) (0.8 unit/μl), and 2.935 μl of distilled water (final volume, 5 μl), was PCR-amplified on a Thermal Cycler Dice (Takara) with the following program; 94°C for 2 minutes (one cycle), 92°C for 20 seconds, 60°C for 3 minutes (35 cycles), held at 4°C. The product was resolved by electrophoresis in 5% agar. A representative result is shown in supplementary Figure S1 (see supplemental Figure S1 at *http://ajp.amjpathol.org*).

Immunohistochemistry

Maximal tumor sections were subjected to immunohistochemistry. Formalin-fixed tissue sections (4 μm thick) were deparaffinized and rehydrated, and incubated with 3% hydrogen peroxide, followed by 5% goat serum to block endogenous peroxidase activities and non-immunospecific protein binding. Antigen retrieval treatment, boiling in citrated buffer (0.01 M/L, pH 6.0), was used for the detection of Ki-67 antigen to restore the masked epitope. Then the sections were incubated with primary antibody against either DUSP6 (Abnova, Taipei, Taiwan) or Ki-67 (MIB1, Dako). Immunoreactivity was visualized with an Envision detection system (Dako), and the nuclei were counterstained with hematoxylin. The specificity of the anti-DUSP6 antibody was confirmed by an experiment with sections cut from paraffin-embedded HEK293T cells that were transfected with the pQCXIP/DUSP6 expression vectors (see supplemental Figure S2 at *http://ajp.amjpathol.org*). Expression levels of DUSP6 in lung cancer cells were subdivided into four categories, negative (0), faint (1), moderate (2), and strong (3). Faint expression was defined as a level similar to that in bronchial epithelial cells. Strong expression was defined as unequivocally greater signal intensity than that of bronchial epithelial cells, and moderate expression was defined as a level in between faint and strong expression. The expression score was determined as the average level. Lung cancers with a score of less than 1, and equal to or more than 1, were classified as reduced expressers and retained expressers, respectively. A labeling index of MIB1 was calculated as a proportion of positive cells by counting 500 to 1000 cancer cells. The lung cancers with a labeling index of less than 0.15 and with 0.15 or more were classified as low and high expressers, respectively.

Loss of Heterozygosity Analysis

H&E-stained tissue sections were checked microscopically. If a tumor was medullary, the tumorous and non-tumorous parts were macroscopically dissected with a razor blade. If a tumor contained abundant interstitial tissue, the tumorous part was captured using the PALM-MCB laser microdissection system (Carl Zeiss, Jena, Germany). The method of DNA extraction from formalin-fixed, paraffin-embedded tissue sections was previously described elsewhere.[2] Loss of heterozygosity (LOH) was evaluated by restriction fragment length polymorphism analysis. Briefly, a 168-bp fragment covering a polymorphic region of exon 1 (340 (t/g); 114 (leucine/valine) was PCR-amplified using 5′-GCGACTGGAACGAGAATACGGG-3′ and 3′- TTTCAATCCACGCGCCCCG-5′, with HotStar Taq polymerase (Stratagene, La Jolla, CA) according to the manufacturer's instruction. Subsequently, the PCR product was digested with BsiHAKI (New England BioLabs), and solved by electrophoresis in 5% agar. In this assay system, only the Leucine allele, but not the Valine allele, is specifically cut into two fragments of 135 and 33 bp.

Search for Mutations

Cells were harvested by trypsinization, and subsequently subjected to DNA extraction as described elsewhere.[2] H&E-stained tissue sections (acetone- or ethanol-fixed, paraffin-embedded tissue) were checked microscopically. If a tumor was medullary, the tumorous and the non-tumorous parts were macroscopically dissected with a razor blade. If a tumor contained abundant interstitial tissue, the tumorous part was captured using the PALM-MCB laser microdissection system (Carl Zeiss, Jena, Germany). The method of DNA extraction from paraffin-embedded tissue section was previously described elsewhere.[2] A fragment of the coding exons (exons 1 to 3) was PCR-amplified using HotStar-TaqDNA polymerase (Stratagene) according to the manufacturer's instruction. PCR products were purified with EXO-SAP-IT (Amersham), and subjected to a dye-terminator reaction using a Big Dye version 3.1 kit (Applied BioSystems, Foster City, CA). Primers used for PCR and DNA sequencing were as described previously.[12]

Statistical Analysis

Differences in cell cycle fractions, DUSP6 expression scores or allelic status among clinicopathologic subgroups were analyzed with Student's *t*-test or the one-way analysis of variance (Game-Howell's test or Tukey's HSD test). The correlation of DUSP6 expression levels with clinicopathologic parameters, *KRAS* gene mutations, MIB index levels, and allelic status was analyzed with Fisher's exact test. *P* values less than 0.05 were considered significant.

Results

Comprehensive Search for Downstream Targets of Oncogenic KRAS

Forced expression of oncogenic KRAS (KRAS/V12) dramatically suppressed the growth of NHBE-T cells (Figure 1, A–D) with flattened and vacuolated morphological changes (Figure 1E). The results led us to expect

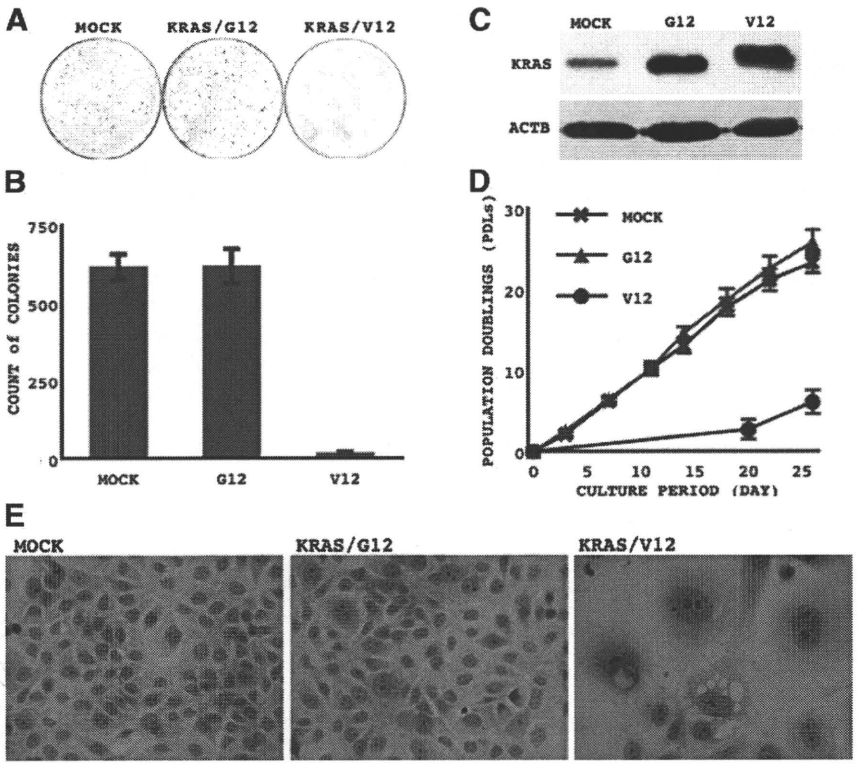

Figure 1. Biological effects of oncogenic KRAS on NHBE-T cells. Empty vector (pQCXIH; MOCK), KRAS/G12 (G12), or KRAS/V12 (V12) was retrovirally transduced into NHBE-T cells. After a 4-day selection process, the surviving populations were harvested and counted, and 1.0×10^4 cells were reseeded onto a 10-cm dish. After 14 days, the cells were fixed with methanol and stained with Giemsa (**A**). The means and standard deviations (error bars) of colony counts from triplicate experiments are presented (**B**). The cells harvested immediately after the selection process were examined for the expression of KRAS and ACTB by Western blotting (**C**). The selected cells were grown and passed several times. The means and standard deviations (error bars) of cumulated PDLs from triplicate experiments are presented (**D**). Cells (2.5×10^4) after the selection process were re-seeded onto chamber slides (LAB-TEK, Electron Microscopy Science; Hatfield, PA) cultured for 48 hours, then fixed with 90% ethanol, and stained with the Papanicolaou method (**E**; ×400).

potential growth suppressor(s) downstream of oncogenic KRAS. A comprehensive evaluation of gene expression revealed the KRAS/V12-transduced cells to have a different expression profile from empty vector (mock)- and KRAS/G12-transduced cells, as the KRAS/V12-transduced cells were classified into the most distant branch on a dendrogram described from a hierarchical clustering analysis (see supplemental Figure S3 at *http://ajp.amjpathol.org*). To identify the factors determining such a difference, we extracted sets of genes up- and down-regulated genes more than fivefold in the KRAS/V12-transduced cells compared with the mock-transduced cells (Table 1 and 2). Among up-regulated genes, DUSP6, a putative negative feedback regulator for the KRAS-ERK pathway, was detected with two independent probes and showed more than a ninefold difference in both. We therefore focused on DUSP6 as a potential suppressor involved in the oncogenic KRAS-induced growth suppression or the carcinogenesis of the lung.

DUSP6 Expression in Immortalized Cells and Cancer Cells

The KRAS/V12-transduced NHBE-T cells showed higher levels of DUSP6 mRNA and protein than either the mock- or KRAS/G12-transduced cells (Figure 2, A–B), confirming the results of the microarray analyses (Table 1 and 2). On the other hand, the lung cancer cells, TKB14, TKB1, TKB2, and TKB8, showed considerably low mRNA levels, less than 0.3-fold that in NHBE-T (Figure 2A; see also supplemental Figure S4 at *http://ajp.amjpathol.org*). Despite having KRAS mutations, A549 and H358 also showed lower mRNA levels (0.15- and 0.7-fold, respectively) than the KRAS/V12-transduced cells (Figure 2A). The protein levels were lower in all lung cancer cell lines examined, except for TKB2, than in NHBE-T (Figure 2C). Interestingly, the levels of mRNA and protein were not parallel, as TKB20 and H1299 cells expressing very high levels of DUSP6 mRNA (about 39- and 13-fold in comparison with NHBE-T, respectively) showed very low protein levels (0.05-fold in TKB20 in comparison with NHBE-T, and undetectable in H1299) (Figure 2, A and C). These findings suggested translational and/or post-translational regulation[23,24] to be one of the mechanisms causing the reduction of DUSP6 protein expression in lung cancer cells.

Effect of DUSP6 on Growth Activity of Immortalized and Cancer Cells

Forced expression of wild-type DUSP6, but not a dominant negative mutant (C293S),[8] markedly suppressed the growth of NHBE-T cells (Figure 3, A–D). A serial transduction of KRAS/V12 markedly suppressed growth also of the C293S-transudced NHBE-T (Figure 3, E and F), although the C293S-transduced cells showed about a 1.5-fold increase in colony formation compared with the mock-transfected cells (Figure 3, E and F). The level of restoration of colony formation by a dominant negative suppression on DUSP6 activity was too small to consider that DUSP6 is an essential factor to induce the growth suppression as downstream target of oncogenic KRAS. Interestingly, KRAS/V12 activated the ERK pathway, as

Table 1. Up-Regulated Genes

Symbol	Genbank	Map	Mock		KRAS/G12		KRAS/V12		Ratio V12/MOCK	Ratio V12/G12
			Signal value	Flags	Signal value	Flags	Signal value	Flags		
PPBP	R64130	4q12-q13	0.06	A	0.10570161	A	24.379782	P	406.3297	230.6472153
NAV3	NM_014903	12q14.3	0.17999999	A	0.30749556	A	32.909496	P	182.8305435	107.0242965
IL1RL1	NM_003856	2q12	0.12306067	A	1	A	17.37906	P	141.2235119	17.37906
ESM1	NM_007036	5q11.2	0.17	A	0.4035879	A	22.06809	P	129.8122941	54.67976121
SERPINB2	NM_002575	18q21.3	0.35317335	P	0.99999994	P	36.968746	P	104.6759219	36.96874822
CCL3	NM_002983	17q11-q21	0.41999996	A	0.93209594	A	43.92214	P	104.5765338	47.12190893
MMP1	NM_002421	11q22.3	0.8234009	P	1	P	82.57412	P	100.2842236	82.57412
NICE-1	NM_019060	1q21	0.95156735	A	1	A	82.501305	P	86.70043692	82.501305
IL24	NM_006850	1q32	0.20504226	P	0.99999994	P	14.915695	P	72.74449179	14.91569589
IL1B	NM_000576	2q14	0.58934176	P	1	P	32.343746	P	54.88113722	32.343746
PI3	NM_002638	20q12-q13	0.27	A	0.32671407	A	14.2768345	P	52.87716481	43.69825426
IL1B	M15330	2q14	0.64027035	P	1	P	23.309114	P	36.40511231	23.309114
S100A7	NM_002963	1q21	0.29999998	A	0.62460035	A	9.610644	P	32.03548214	15.38686938
HSD17B2	NM_002153	16q24.1-q24.2	0.16	A	0.23062168	A	5.040771	P	31.50481875	21.85731628
FOS	BC004490	14q24.3	0.48000002	A	0.9513144	A	11.526349	P	24.01322608	12.11623518
STEAP	NM_012449	7q21	0.43252343	P	1	P	7.8730335	P	18.20255957	7.8730335
DUSP6	BC003143	12q22-q23	0.8425659	P	1	P	12.893464	P	15.30261787	12.893464
EGR3	NM_004430	8p23-p21	0.49825794	A	1	A	6.581242	P	13.20850401	6.581242
MMP3	NM_002422	11q22.3	0.8211574	P	1	P	10.295607	P	12.53792148	10.295607
SCG2	NM_003469	2q35-q36	0.607316	P	1	P	7.09176	P	11.67721582	7.09176
KRTHA4	NM_021013	17q12-q21	0.6581211	P	1	P	7.3771305	P	11.20938153	7.3771305
DUSP6	BC003143	12q22-q23	0.9104498	P	1	P	9.899106	P	10.87276421	9.899106
CSF2	M11734	5q31.1	0.82838905	P	1	P	8.029184	P	9.692527925	8.029184
CXCL2	M57731	4q21	0.7698449	P	1	P	6.89791	P	8.960129501	6.89791
EGR1	NM_001964	5q31.1	1.7957487	P	1.3774424	P	12.828883	P	7.144030231	9.313553147
MME	NM_007287	3q25.1-q25.2	0.83048177	P	1	P	5.7785997	P	6.958129496	5.7785997
GEM	NM_005261	8q13-q21	0.5474987	A	0.99999994	P	3.7885349	P	6.919714878	3.788535127
DOCK4	NM_014705	7q31.1	0.9751374	P	1	P	6.589132	P	6.757131867	6.589132
BMP2	AA583044	20p12	0.77180034	A	1	A	5.088037	P	6.592426482	5.088037

Mock, empty vector-transduced; KRAS/G12-transduced; KRAS/V12-transduced NHBE-T cells; Symbol, gene name; Map, Chromosomal locus; Genbank, gene bank accession number. Flags indicate whether gene expression is present (P) or absent (A).

well as suppressed growth, and C293S further activated ERK in a dominant negative manner (Figure 3G), but did not enhance the KRAS-induced growth suppression. Therefore, it was speculated that oncogenic KRAS could modulate targets other than the ERK1/2 pathway for the growth suppression. On the other hand, the surviving subpopulations generated from the KRAS/V12-transduced cells (MOCK/V12 in Figure 3H) were no more

Table 2. Down-Regulated Genes

Symbol	Genbank	Map	Mock		KRAS/G12		KRAS/V12		Ratio V12/MOCK	Ratio V12/G12
			Signal value	Flags	Signal value	Flags	Signal value	Flags		
CMKOR1	AI817041	2q37.3	2.897788	P	1	A	0.13582303	A	0.046871279	0.13582303
STS	NM_000351	xp22.32	3.4030955	P	1	A	0.19202565	A	0.056426759	0.19202565
CCL2	S69738	17q11.2-q21.1	2.5081918	P	1	P	0.14537899	P	0.057961672	0.14537899
SCAND2	NM_022050	15q25-q26	0.38724586	P	0.18206042	A	0.023738872	A	0.06130181	0.130390076
SCAND2	NM_022050	15q25-q26	2.1270185	P	1	A	0.13039011	A	0.061301822	0.13039011
PDGFRL	NM_006207	8p22-p21.3	1.8670229	P	1	P	0.12245405	A	0.065587867	0.12245405
COL5A1	AI130969	9q34.2-q34.3	1.3539611	P	0.99999994	P	0.09460237	P	0.069870818	0.094602376
ITPR2	AI963873	12p11	4.62	P	0.7495205	A	0.35317504	A	0.076444814	0.471201308
TSPAN-2	BF129969	1p13.1	1.825053	P	1	P	0.14110127	P	0.077313519	0.14110127
LASS4	NM_024552	19p13.3	0.97412205	P	0.7371226	A	0.07814046	A	0.080216293	0.106007413
EPHA4	NM_004438	2q36.1	3.301421	P	1	A	0.2928391	A	0.088700926	0.2928391
NEDD9	AL136139	6p25-p24	1.4222593	P	1	P	0.1354199	P	0.095214635	0.1354199
NEDD9	U64317	6p25-p24	2.1407213	P	1	P	0.20491455	A	0.095722199	0.20491455
METAP2	NM_006838	12q23.1	1.5916058	P	0.99999994	P	0.15723512	A	0.098790241	0.157235129
HOXC8	NM_022658	12q13.3	0.4796673	P	0.46980467	A	0.04846686	A	0.10104266	0.103163853
SGEF	AU118383	3q25.2	2.7925768	P	1	A	0.28845292	A	0.103292744	0.28845292
MEST	NM_002402	7q32	1.0919998	P	1	P	0.12080742	P	0.110629526	0.12080742
	M78162		2.2374306	P	1	A	0.25059348	A	0.11200056	0.25059348
RHOBTB3	N21138	5q15	1.592752	P	1	P	0.17884138	P	0.112284511	0.17884138
MARCKS	AW163148	6q22.2	1.7614398	P	1	P	0.19830465	A	0.112580998	0.19830465
PAPSS2	AW299958	10q23-q24	1.7204325	P	1	P	0.20847437	P	0.121175559	0.20847437
OLR1	AF035776	12p13.2-p12.3	1.2022126	P	0.99999994	P	0.15065517	P	0.125314915	0.150655179
GALNT4	NM_003774	12q21.3-q22	4.326977	P	0.99999994	A	0.5778095	A	0.133536531	0.577809535
FBLN1	Z95331	22q13.31	1.1362673	P	1	P	0.16118747	P	0.141857	0.16118747
FGL2	NM_006682	7q11.23	2.5700002	P	0.55733573	A	0.3745796	A	0.145750806	0.672089694
NR2F1	AI951185	5q14	1.3209105	P	1	P	0.19696297	P	0.149111518	0.19696297
NR2F1	AI951185	5q14	5.6848426	P	4.3037305	P	0.84767556	P	0.149111527	0.196962974
SYCP1	NM_003176	1p13-p12	2.3125896	P	0.99999994	A	0.3712496	A	0.160534148	0.371249622
TNFSF10	AW474434	3q26	2.61	P	0.6342096	A	0.43879327	A	0.168120027	0.691874216
SCNN1A	NM_001038	12p13	2.845504	P	1	P	0.48475575	A	0.170358485	0.48475575

Mock, empty vector-transduced; KRAS/G12-transduced; KRAS/V12-transduced NHBE-T cells; Symbol, gene name; Map, Chromosomal locus; Genbank, gene bank accession number. Flags indicate whether gene expression is present (P) or absent (A).

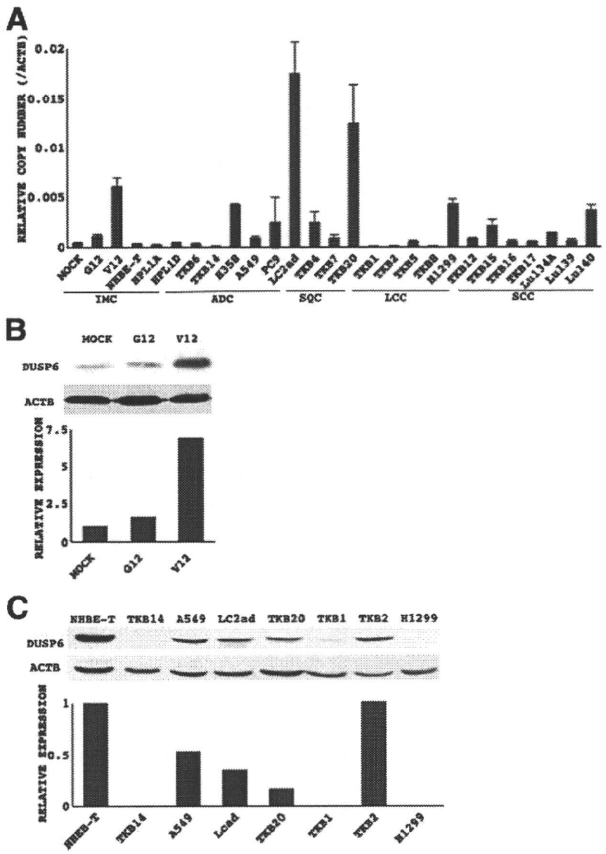

Figure 2. Expression of DUSP6 in immortalized and cancer cell lines. Copy numbers of DUSP6 and ACTB mRNA were measured by quantitative reverse transcription-PCR. The means and standard deviations (error bars) of the mRNA expression of DUSP6 normalized to that of ACTB obtained from triplicate experiments are presented (**A**). DUSP6 and ACTB protein expression in immortalized (**B, upper panel**) and lung cancer cells (**C, upper panel**) was analyzed by Western blotting. Representative results are shown. Levels of DUSP6 and ACTB protein were semiquantified with a densitometer (NIH Image; National Institute of Mental Health at Bethesda, MD). The protein expression of DUSP6 was normalized to that of ACTB. The expression level relative to that in MOCK (**B, lower panel**) to NHBE-T (**C, lower panel**) cells is presented. IMC, immortalized airway cells; MOCK, empty vector-transduced NHBE-T; G12, KRAS/G12-transduced NHBE-T; V12, KRAS/V12-transduced NHBE-T; adenocarcinoma, ADC; squamous cell carcinoma, SQC; large cell carcinoma, LCC; small cell carcinoma, SCC.

affected with the growth suppression, suggesting that the surviving subpopulation potentially having some (epi-) genetic alterations, which made the cells resistant to the KRAS/V12-induced suppression, was selected. Moreover, the surviving subpopulations generated from the C293/V12-transduced cells exhibited gain of anchorage-independent activity in soft agar (Figure 3, I and J; see also supplemental Figure S5 at *http://ajp.amjpathol.org*), although no enhancement in growth activity was observed under anchorage-supplied culture conditions (on the ordinary poly-L-lysine-coated plastic dish) (Figure 3H). The result indicated that DUSP6's inactivation further conferred a growth advantage to the subpopulation surviving from the oncogenic KRAS-induced growth suppression under the specific condition, implying that DUSP6's inactivation might be involved especially in the progression process of KRAS-mediated carcinogenesis. Actually, forced expression of DUSP6 markedly suppressed the growth of A549, a lung cancer cell line bearing a KRAS mutation (G12S) (Figure 4, A–D), and significantly attenuated the incorporation of BrdU (Figure 4E, upper panel; Table 3). The result of the flow cytometric analysis that the fractions at S phase decreased and those at G1 phase increased confirmed the former observation (Figure 4E, lower panel; Table 3). No sub-G1 fraction, which indicates the induction of apoptosis, was observed (Figure 4E, lower panel; Table 3). Similar results were obtained from experiments with H1299 and TKB1, a cell line without KRAS mutations (see supplemental Figure S6 at *http://ajp.amjpathol.org*). Taken together, these results suggested that DUSP6 could function as a growth suppressor by preventing cell cycle progression and implied that it could prevent carcinogenesis of the lung with or without KRAS mutations. However, exogenously transduced genes often induce artificial phenotypes due to the excessive amount not being physiologically relevant. So, we checked levels of expression of exogenously transduced DUSP6 in the cancer cell lines and compared these with a level of endogenous expression in NHBE-T. The levels of exogenous expressions in the cancer cell lines were higher than that of endogenous expression in NHBE-T, but seemed not far excessive (see supplemental Figure S7 at *http://ajp.amjpathol.org*), although it may be impossible to exactly judge whether such levels of the exogenous expression were physiologically relevant or not. It is a limitation of the transduction experiments. We, therefore, performed a knockdown experiment on NHBE-T and A549 cells to further verify a potential significance of the DUSP6's down-regulation in the KRAS/V12-induced growth suppression and in the biological properties of cancer cells using a stable siRNA expression system. However, we did not obtain the expected result in its effect of on KRAS/V12-induced growth suppression, and growth activity of NHBE-T in ordinary culture and in soft agar (see supplemental Figure S8 at *http://ajp.amjpathol.org*). Also, we failed to find any significant change in growth activity of A549 cells in ordinary culture and in soft agar (data not shown). This inconsistency was speculated to be due to a level of reduction too small to exhibit significant change in biological activity, as an efficiency of the knockdown seemed not enough to overcome the KRAS-mediated up-regulation of DUSP6 expression (see supplemental Figure S8 at *http://ajp.amjpathol.org*). To verify more satisfactorily significances of DUSP6 in the oncogenic KRAS-induced growth suppression and in the biological properties of cancer cells, further improvement of experimental system might be required.

Deficiency of Oncogenic KRAS-Mediated Transactivation and Translation of DUSP6 in Lung Cancer Cells

Exogenous expression of KRAS/V12 only slightly modulates DUSP6 expression at the mRNA or protein levels in either A549 (KRAS-mutated) or H1299 cells (KRAS-intact) (see supplemental Figure S9 at *http://ajp.amjpathol.org*), suggesting transcriptional and/or translational deficiency to be

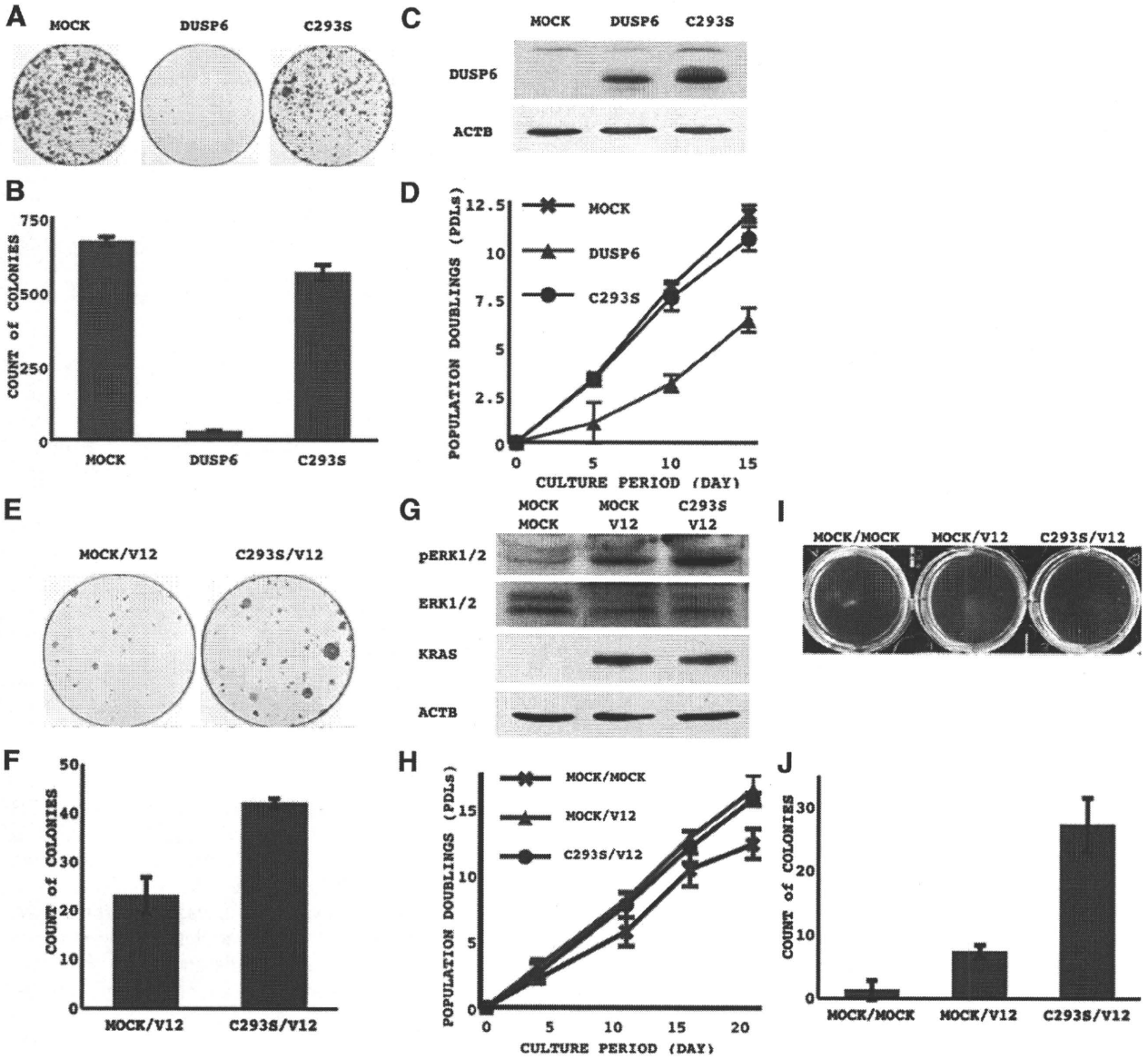

Figure 3. Biological effects of DUSP6 on NHBE-T cells. Empty vector (pQCXIP; MOCK), DUSP6, or DUSP6/C293S (C293S)[8] was retrovirally transduced into NHBE-T cells. Three days after selection with puromycin, the surviving cells were harvested and counted, and 1.0×10^4 cells were re-seeded onto a 10-cm dish. After 14 days, the cells were fixed with methanol and stained with Giemsa (**A**). The means and standard deviations (error bars) of colony counts from triplicate experiments are presented (**B**). The cells harvested immediately after the selection process were examined for expression of DUSP6 and ACTB by Western blotting (**C**). The cells after the selection process were grown and passed several times. The means and standard deviations (error bars) of cumulated PDLs from triplicate experiments are presented (**D**). The puromycin-selected MOCK- and DUSP6/C293 (C293)-transduced cells were serially transduced with KRAS/V12 (V12). Three days after selection with hygromycin B, the cells were harvested and counted, and 5.0×10^4 cells were re-seeded onto a 10-cm dish. After 14 days, the cells were fixed with methanol and stained with Giemsa (**E**). The means and standard deviations (error bars) of counts of colonies visible in scanned photographs from triplicate experiments are presented (**F**). The subpopulations generated from the MOCK/V12- or C293S/V12- serially transduced NHBE-T cells and the empty pQCXIP/pQCXIH-transduced NHBE-T cells (MOCK/MOCK) were examined for the expression of phosphorylated ERK1/2 (pERK1/2), ERK1/2, KRAS, and ACTB by Western blotting. Representative results are shown (**G**). The subpopulations were grown and passed several times under ordinal culture conditions. The means and standard deviations (error bars) of cumulated PDLs from triplicate experiments are presented (**H**). Cells (1.25×10^4) of the subpopulations were cultured and grown in 0.3% soft agar for 5 weeks, then fixed with a buffered 4% paraformaldehyde solution (**I**). The means of colony counts and standard deviations (error bars) from triplicate experiments are presented (**J**).

one of the mechanisms involved in the reduction of DUSP6 expression observed in lung cancer cells.

Analysis of CpG Methylation in the DUSP6 Promoter

Treatment with a DNA methyl-transferase inhibitor (AZA) alone, or in combination with a histone deacetylase (TSA), restored DUSP6 mRNA expression in all of the cancer cell lines examined, although the extent of restoration differed among the cells (Figure 5A). In NHBE-T, however, TSA-treatment, but not AZA-treatment, restored the expression, and the combination had no more of an effect than TSA alone (Figure 5A). These results implied the involvement of the promoter's hypermethylation (and/or histone deacetylation) in the pathological sup-

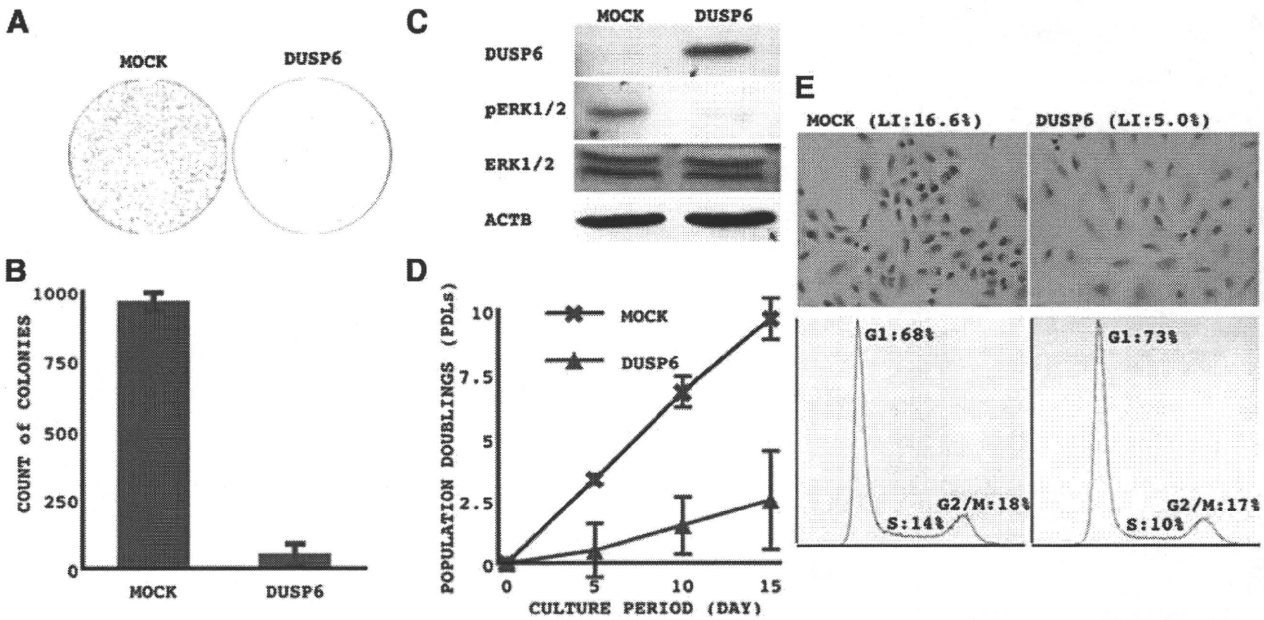

Figure 4. Biological effects of DUSP6 on A549 lung cancer cells. Empty vector (pQCXIP; MOCK) or DUSP6 was retrovirally transduced into A549 cells. Three days after the selection process, cells were harvested and counted, and 1.0×10^4 cells were re-seeded onto a 10-cm dish. After 12 days, the cells were fixed with methanol and stained with Giemsa (**A**). The means and standard deviations (error bars) of colony counts from triplicate experiments are presented (**B**). The cells harvested immediately after the selection process were examined for the expression of DUSP6 and ACTB by Western blotting. Representative results are shown (**C**). The selected cells were cultured, grown, and passaged. The means and standard deviations (error bars) of cumulated PDLs from triplicate experiments are presented (**D**). The cells (2.5×10^4) were seeded onto chamber slides (LAB-TEK 2-well chamber, Electron Microscopy Science) and cultured for 48 hours, then pulse-labeled with BrdU, fixed, and immunostained for BrdU for determining a labeling index (**E, upper panels**; LI, BrdU labeling index). The cells (2.5×10^5) after the selection process were seeded onto a 10-cm dish and grown for 5 days, then harvested and fixed with 70% ethanol, and subjected to RNase A treatment. The cells were stained with propidium iodide, and cell cycle fractions were analyzed with a flow cytometer (**E, lower panels**).

pression of DUSP6 transcription in the lung cancer cells, but not necessarily in its regulation in NHBE-T. To test this notion, we attempted to determine the promoter region of DUSP6. The results of luciferase reporter assays indicated that the promoter region lay between −1030 and +24 with strong elements between −1030 and −510, as the construct bearing −1030 to +24 showed markedly greater reporter activity than that bearing −511 to + 24 (Figure 5B). On the other hand, an in silico analysis using computer software (Genomatix, Munichi, Germany), indicated that the promoter was within the locus from −960 to −266, well consistent with the murine DUSP6 promoter demonstrated by Ekerot et al.[6] We thus focused on this locus and searched for CpG methylation by bisulfate conversion-based DNA sequencing. Unexpectedly, almost all of the CpG sites were unmethylated in the cell lines examined (Figure 5C). We further examined the cell lines for methylation at the locus from +544 to +627, where a significant association between methylation status and mRNA expression was reported in pancreatic cancers.[16] We used the same methylation-specific PCR analysis that was described previously.[16] Although this locus was methylated in some lung cancer cell lines (Figure 5D), no correlation between the methylation status and DUSP6 mRNA expressions was found (Figure 2A and Figure 5D). We therefore speculated that the restoration of mRNA expression mediated by the inhibitors (Figure 5A) could be a secondary event resulting from the restoration of silenced potential transactivators, changes in the modification of histones, or other factors involved in the transcription process, although the involvement of hypermethylation of another site on the DUSP6 gene locus was not completely excluded.

Table 3. Effect of DUSP Expression on Cell Cycle Progression

	Mock	DUSP6	*P* value
sub-G1	0.0 ± 0.0	0.0 ± 0.0	1.000
G1	66.4 ± 1.9	73.9 ± 1.0	0.048
S	15.5 ± 1.0	8.9 ± 1.1	0.031
G2/M	17.1 ± 1.2	18.1 ± 1.0	0.330
BrdU Index	16.5 ± 0.7	5.6 ± 1.3	0.011

Mock, empty vector-transduced; DUSP6, DUSP6-transduced cells. Mean± Standard deviation from three independent experiments is shown; *P* value calculated with Student's *t*-test.

DUSP6 Expression in Primary Lung Cancers

For 96 cases of primary lung cancer, DUSP6 expression was examined by immunohistochemistry, and the correlation with growth activity, KRAS mutations, and other pathological parameters, was analyzed. DUSP6 expression was semiquantified according to the scoring system described in the *Materials and Methods*. The growth activity was evaluated as a MIB1 labeling index. Representative results of immunohistochemistry for DUSP6 and Ki-67 (MIB1) are shown in Figure 6. Statistical analysis revealed a significant inverse correlation between DUSP6 expression and growth activity (Table 4) (confirmed with Spearmen's correlation test; $\rho = -0.324$, $Z = -3.141$, $P = 0.0016$). Significant inverse correlations were also

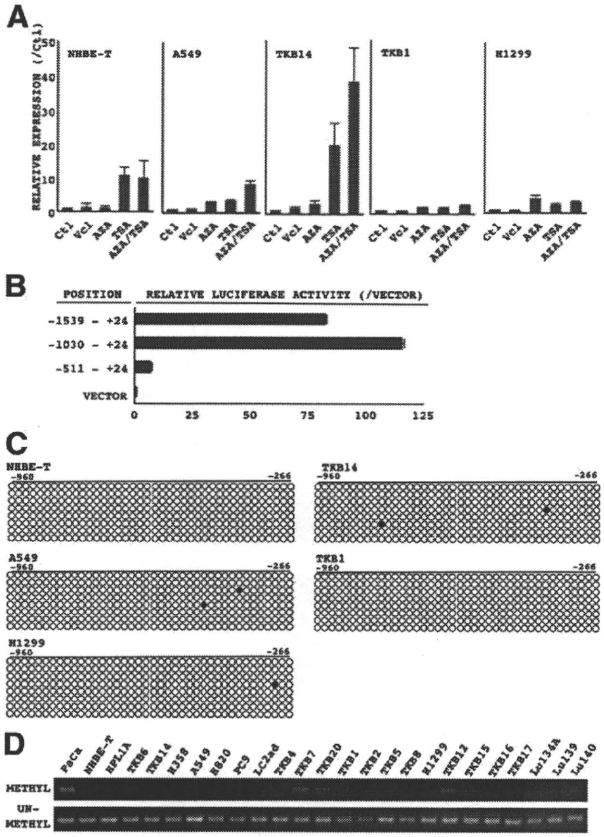

Figure 5. Methylation status of the DUSP6 promoter and intron 1. Cells treated with vehicle (Vcl), AZA, TSA, or a combination of AZA and TSA were examined for restoration of DUSP6 mRNA expression by quantitative reverse transcription-PCR. The copy number of DUSP6 mRNA normalized to that of β-actin was determined as the DUSP6 expression level in each cell sample. Then, relative expression normalized to the level of the untreated control (Ctl) in each cell line that was obtained from triplicate experiments, are plotted (*y* axis) (**A**). Luciferase reporter constructs, empty vector, −511 to +24, −1030 to +24, and −1539 to +24 (position of the first base of the start codon was determined as +1), were transfected into NHBE-T. Luciferase activities were measured and normalized as described in the *Materials and Methods*. The means and standard deviations (error bars) of the ratio of activity to that for empty vector (VECTOR) from duplicated experiments are presented (**B**). The region from −960 to −266 in the DUSP6 gene locus was PCR-amplified using sodium bisulfate-modified genomic DNA as a template. Eight subclones of PCR products were analyzed for methylation status by DNA sequencing. Open (○) and filled (●) circles indicate un-methylated and methylated cytosine at indicated CpG sites, respectively (**C**). The region from +544 to +627 in intron 1 of the DUPS6 gene was PCR-amplified with primers specific for either methyl or un-methyl DNA[16] using sodium bisulfate-modified genomic DNA as a template. The products were resolved by electrophoresis in 3% agar and stained with ethidium bromide (**D**).

observed between DUSP6 expression and the histological grade of ADC, T factor, and stage (Table 4). No difference in DUSP6 expression was found between cases with and without KRAS mutations (Table 4).

Allelic Imbalance of the DUSP6 Locus in Primary Lung Cancers

Among 121 cases examined, 64 cases (52.8%) were heterogeneous and informative, 22 cases (18.2%) were homozygous having the leucine allele, and 35 cases (28.9%) were homozygous having the valine allele. The allele frequency was 44.6% and 55.4% in the leucine and valine type, respectively. Among the informative cases (46 ADC, 16 SQC, and 2 LCC), LOH, evaluated by restriction fragment length polymorphism analysis, was found in 11 cases (17.2%; 10 ADC, 1 SQC, 0 LCC) (Table 5). A representative result of the restriction fragment length polymorphism analysis is shown in Figure 7. Analysis of the correlation between allelic status and immunohistochemical expression of DUSP6 revealed tumors with LOH to have significantly weaker expression than those without LOH, especially in adenocarcinomas (Table 5). No statistically significant association was found with the other analytical subjects, including histological type (ADC [21.7%, 10/46], SQC [6.3%, 1/16], LCC [0.0%, 0/2]; Fisher's exact test, $P = 0.2972$), stage (1A [13.9%, 5/36], 1B [15.3%, 2/13], 2B [25.0%, 1/4], 3A [14.2%, 1/7], 3B [50.9%, 2/4]; Fisher's exact test, $P = 0.4712$), MIB1 index (LOH 0.184 ± 0.216, retained 0.234 ± 0.219; Student's *t*-test, $P = 0.4966$), and so on (data not shown).

Gene Mutation in the Protein-Coding Exons of DUSP6 Gene

Among 21 lung cancer cell lines (described in the *Materials and Methods*) and 48 primary lung cancers (36 ADC, 10 SQC, and 2 LCC) examined, no novel base substitution or deletion was found (data not shown), although known genetic polymorphisms were seen in some of the cancer cell lines and primary lung cancers (data not shown).

Discussion

It has been generally accepted that *RAS* is an oncogene, as innumerable studies reproducibly demonstrated that mutated *RAS* (either *KRAS* or *HRAS*) provided immortalized murine fibroblastic cells (NIH3T3) with malignant phenotypes such as contact inhibition-ignoring and anchorage-independent growth activities, or tumorigenicity in immunodeficient animals.[4,25,26] However, mutated RAS (HRAS/V12) has been known to induce severe growth suppression, regarded as premature senescence, in some types of cells, such as early-passage murine and human fibroblasts,[27–29] and small airway epithelial cells.[2] The present study demonstrated a similar event in the KRAS/V12-transduced NHBE-T cells (Figure 1E). Previous studies reported p16INK4A and/or p14ARF, transactivated by ETS2 and/or DMP1 through the RAS-ERK (or-p38MAPK) pathway, to be essential effectors inducing premature senescence, as confirmed by the findings that a blockade of the p16INK4A/RB and/or p14ARF/p53 pathways by E1A (adenovirus) or large T (Simian virus 40) antigens eliminated this event.[27–32] The NHBE-T used in this study, however, is Simian virus 40-immortalized, expressing large T antigens. The KRAS/V12-induced growth suppression seemed a novel event different from so-called premature senescence. We therefore examined other cell lines for this event. Transduction of KRAS/V12 induced severe growth suppression in the cells without *KRAS* mutations (H1299 [p53-inactivated, p16-inacti-

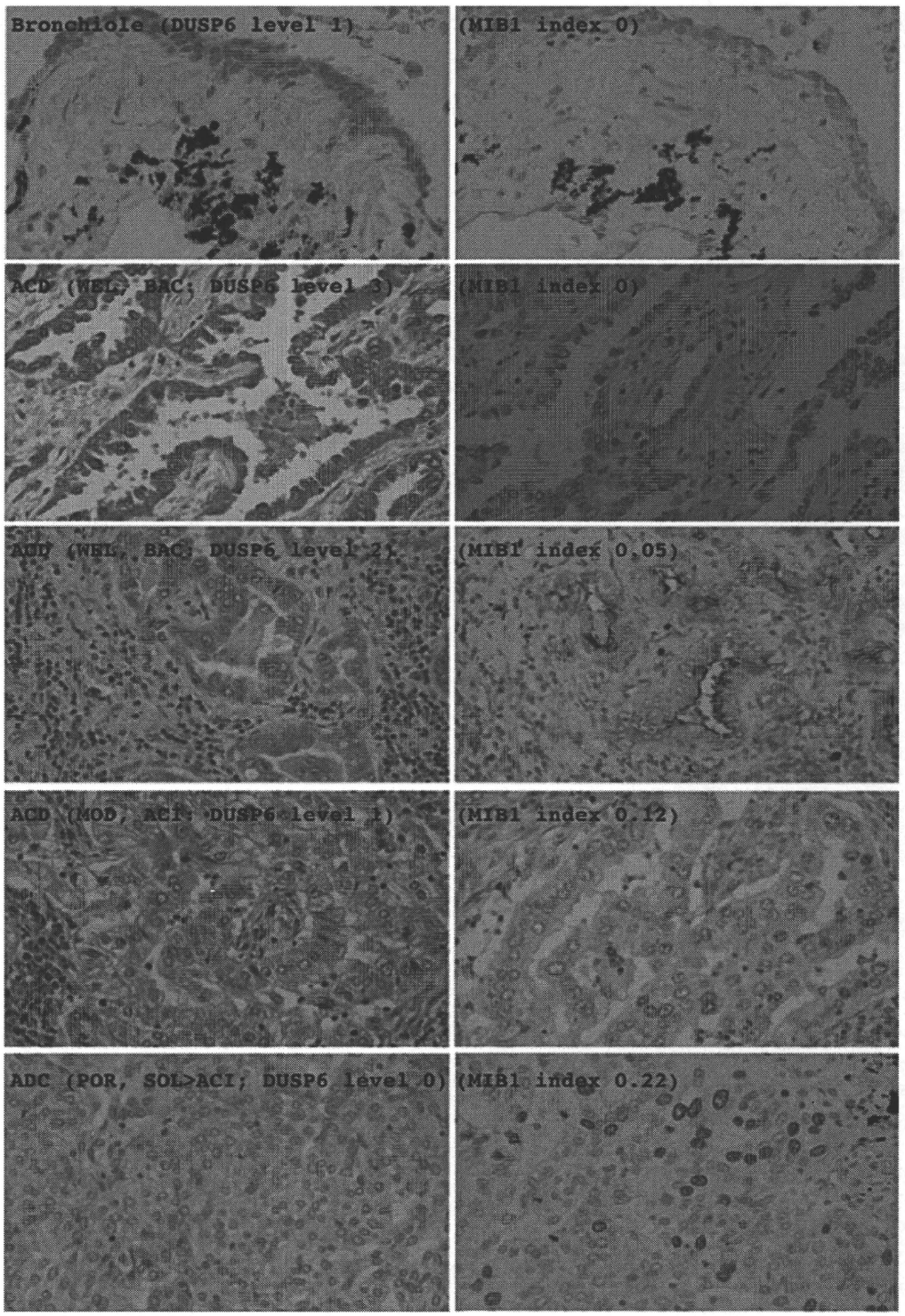

Figure 6. Expression of DUSP6 and Ki-67 in primary lung cancers. The expression of DUSP6 (**left** panels) and Ki-67 (MIB1, **right** panels) in normal bronchial epithelia and primary lung cancers was examined by immunohistochemistry. Levels of DUSP6 expression were subdivided into four categories; negative (level 0, **left bottom panel**), faint (level 1, **left fourth panel**), moderate (level 2, **left third panel**), and strong (level 3, **left second panels**). Faint expression was defined as a level similar to that of bronchial epithelial cells (**left top** panel). Strong expression was defined as unequivocally greater signal intensity than that of bronchiolar epithelial cells (**left second panel**), and moderate expression was defined as a level in between faint and strong (**left fourth panel**). Proportions of Ki-67-expressing cells were determined as a labeling index of MIB1 (MIB1 index) as described in the *Materials and Methods*. ADC, adenocarcinoma; WEL, well differentiated; MOD, moderately differentiated; BAC, bronchioloalveolar carcinoma; ACI, acinar carcinoma; SOL, solid carcinoma with mucin. Magnification is × 400 for each.

Table 4. Correlation between DUSP6 Expression and Clinicopathologic Status in Primary Lung Cancers

	Reduced (Score <1)	Retained (Score >1)	Score ($M \pm SD$)
*MIB1 Labeling Index (96)			
Low Level (<15%) (34)	6 (17.6%)	28 (82.4%)	1.416 ± 0.564†
High Level (≥15%) (62)	37 (59.7%)	25 (40.3%)	0.898 ± 0.536†
KRAS Codon12 (90)			
Mutant type (22)	8 (36.4%)	14 (63.6%)	1.119 ± 0.693
Wild-type (68)	32 (47.1%)	36 (52.9%)	1.057 ± 0.575
*Histology (96)			
ADC (65)	18 (27.7%)	47 (72.3%)	1.272 ± 0.558‡
*Grade			
WEL (37)	5 (13.5%)	32 (86.5%)	1.446 ± 0.506‡
MOD (20)	8 (40.0%)	12 (60.0%)	1.075 ± 0.521
POR (8)	5 (62.5%)	3 (37.5%)	0.869 ± 0.548‡
Subtype			
BAC (35)	6 (25.7%)	29 (74.3%)	1.458 ± 0.433
ACI (11)	4 (36.4%)	7 (63.6%)	0.982 ± 0.541
PAP (12)	4 (16.7%)	8 (83.3%)	1.183 ± 0.242
SOL (7)	3 (42.9%)	4 (57.1%)	0.950 ± 0.492
SQC (26)	21 (80.8%)	5 (19.2%)	0.754 ± 0.451‡
Grade			
WEL (6)	5 (16.7%)	1 (83.3%)	0.750 ± 0.464
MOD (16)	13 (81.3%)	3 (18.7%)	0.660 ± 0.457
POR (4)	3 (75.0%)	1 (25.0%)	1.100 ± 0.606
LCC (5)	4 (80.0%)	1 (20.0%)	0.310 ± 0.486‡
*T Factor (96)			
T1 (36)	10 (27.8%)	26 (72.2%)	1.274 ± 0.625§
T2 (41)	21 (48.8%)	20 (51.2%)	1.012 ± 0.640
T3 (6)	3 (50.0%)	3 (50.0%)	1.133 ± 0.383
T4 (13)	10 (76.9%)	3 (23.1%)	0.746 ± 0.288§
N Factor (96)			
N0 (61)	22 (36.1%)	39 (63.9%)	1.148 ± 0.637
N1 (11)	7 (63.6%)	4 (36.4%)	0.955 ± 0.468
N2 (18)	10 (55.6%)	8 (44.4%)	0.939 ± 0.609
N3 (6)	4 (66.7%)	2 (33.3%)	1.067 ± 0.476
*Stage (96)			
1A (31)	6 (19.4%)	25 (80.6%)	1.350 ± 0.587¶
1B (25)	14 (56.0%)	11 (44.0%)	0.891 ± 0.659
2A (2)	2 (100.0%)	0 (0.0%)	0.500 ± 0.283
2B (10)	4 (40.0%)	6 (60.0%)	1.180 ± 0.454
3A (10)	4 (40.0%)	6 (60.0%)	1.140 ± 0.509
3B (16)	12 (75.0%)	4 (25.0%)	0.831 ± 0.406¶
4 (2)	1 (50.0%)	1 (50.0%)	1.100 ± 0.283

*$P < 0.005$, Fisher's exact test; †$P < 0.001$, Student's t-test; ‡$P = 0.001$, Tukey's HSD test; §$P = 0.001$, Games-Howell's test; ¶$P = 0.0012$ Games-Howell's test. ADC, adenocarcinoma; SQC, squamous cell carcinoma; LCC, large cell carcinoma; WEL, well differentiated; MOD, moderately differentiated; POR, poorly differentiated carcinomas; BAC, bronchioalveolar carcinoma; ACI, aciner adenocarcinoma; PAP, papillary adenocarcinoma; SOL, solid adenocarcinoma with mucin production.

vated, KRAS-intact, see supplemental Figure S10 at *http://ajp.amjpathol.org*], TKB1 [p53-inactivated, p16-inactivated, KRAS-intact, data not shown], and primary small airway epithelial cells, data not shown), but only modest suppression in the cells with KRAS mutations (A549 [p53-intact, p16-inactivated, KRAS-mutated, see supplemental Figure S11 at *http://ajp.amjpathol.org*] and H358 [p53-inactivated, p16inactivated, KRAS-mutated, data not shown]). These results indicated that the KRAS/V12-induced growth suppression was not unique to NHBE-T, suggested the p16INK4A/RB and/or p14ARF/p53 pathways not to be essential for such suppression,

Table 5. Correlation between DUSP6 Allelic Status and Expression

	RTN	LOH	*P* value
Whole (64)	1.158 ± 0.664 (53)	0.755 ± 0.664 (11)	0.182
ADC (46)	1.542 ± 0.664 (36)	0.820 ± 0.664 (10)	0.022
SQC (16)	0.327 ± 0.094 (15)	0.110 ± 0.000 (1)	NA
LCC (2)	0.500 ± 0.707 (2)	NA	NA

RTN, retained; LOH, loss of heterozygosity; NA, not available; ADC, adenocarcinoma; SQC, squamous cell carcinoma; LCC, large cell; LCC, large cell carcinoma; (), indicates number of cases. *P* value calculated with Student's *t*-test.

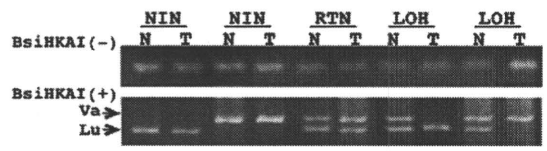

Figure 7. LOH analysis. A 168-bp fragment covering a polymorphic region of exon 1 (340 (t/g); 114 (leucine/valine) was PCR-amplified, subsequently digested with BsiHAKI, and then solved by electrophoresis in 5% agar. The leucine allele (Lu) is cut into 135 (and 33) −bp fragments (faster migrating band). The valine allele is resistant to BsiHAKI digestion (slower migrating band). A representative result is shown. **Upper panel**, without BsiHAKI digestion; **lower panel**, with BsiHAKI digestion. NIN, not informative (homozygous); RTN, allele is retained; LOH, loss of hemi allele; N, non-tumoral part; T, tumoral part.

and implied that only clones overcoming suppression would be able to develop into lung cancers having KRAS mutations. Therefore, it would be of great interest to identify the effector(s) inducing such growth suppression, because they could be potential tumor suppressors playing crucial role(s) in oncogenic KRAS-mediated carcinogenesis, especially at the initiating step. A comprehensive search for downstream targets of oncogenic KRAS (KRAS/V12) uncovered several candidates (listed in Tables 1 and 2). The present study focused on DUSP6, but failed to prove it indispensable to induce oncogenic KRAS-induced growth suppression, since a dominant negative DUSP6 (C293S) failed to rescue the suppression significantly (Figure 3, E–G), and oncogenic KRAS did not increase DUSP6 expression despite the induction of growth suppression in H1299 cells (see supplemental Figure S9 at *http://ajp.amjpathol.org*). The potential involvement of the other factors listed in the tables is currently being investigated in detail. On the other hand, the subpopulation generated from NHBE-T serially transduced with a dominant-negative DUSP6 (C293S) and KRAS/V12 acquired higher anchorage-independent growth activity than that generated from cells transduced with KRAS/V12 alone (Figure 3, I and J, see also supplemental Figure S5 at *http://ajp.amjpathol.org*), suggesting that DUSP6 promotes the progression of lung carcinogenesis by maintaining stable activation of the ERK-mediated oncogenic pathway. The observations that forced expression of DUSP6 markedly suppressed the growth of lung cancer cell lines (Figure 4; see supplemental Figure S6 at *http://ajp.amjpathol.org*) and that the expression decreased with an increase in growth activity, as well as the progression of grade and stage of lung cancers (Figure 6 and Table 4) support our notion. Interestingly, early stage or low-grade lesions tended to express DUSP6 at high levels compared with the normal bronchial epithelia (Figure 6 and Table 4). This finding was comparable with previous observations in pancreatic cancers.[13,14] Both in the lung and in the pancreas, KRAS mutations are very early events, which can be found even in premalignant lesions.[1,2,15] It is supposed that premalignant or early lesions still maintain a DUSP6-mediated negative feedback response that interferes with oncogenic stimuli from mutated KRAS. However, in lung cancers, *KRAS* mutations are not so frequent, and found only in 5% to 30% of cases.[1,2,33] As a substitute for *KRAS* mutations, either *EGFR* or *BRAF* oncogenes are mutated mutually exclusively in 10% to 50%[34,35] and 0% to 3%[34] of cases, respectively. Mutations in any of these three oncogenes are estimated to occur in up to 80% of lung cancers. *EGFR*, *KRAS*, and *BRAF* activate a common signaling pathway in this order, which subsequently activates the MEK-ERK cascade.[36] Thus, oncogenic stimuli from EGFR, KRAS, or BRAF potentially excite a DUSP6-mediated negative-feedback response in the same way. Actually, a previous report demonstrated that DUSP6 was also transactivated by transduction of an oncogenic mutant of EGFR.[4] This observation suggests that DUSP6 acts as a growth suppressor not only in oncogenic KRAS-mediated carcinogenesis, but also in EGFR- (and BRAF)-mediated carcinogenesis. The result that DUSP6 levels did not differ between the lung cancers with KRAS mutations and those without KRAS mutations (Table 4) seems supportive of this notion.

Aside from the role of DUSP6 in carcinogenesis of the lung, we tried to elucidate the mechanisms mediating the reduction of its expression. The methylation status of the promoter region and intron 1 (+544 to +627),[16] mutations in the coding exons, and allelic imbalance (LOH) were investigated, because these are pivotal mechanisms inactivating many known tumor suppressors.[37] We, however, failed to find hypermethylation of the promoter, a correlation between the methylation status of intron 1 and the expression, or mutations, in any of the lung cancer cell lines (Figure 5). Therefore, we have considered that hypermethylation, at least of the regions examined here, and gene mutation are not the major cause of the down-regulation of DUSP6 expression in lung cancers. On the other hand, LOH was found in 17.2% of primary lung cancers and was inversely associated with DUSP6 expression in ADC (Figure 7 and Table 5), suggesting LOH to be one of the mechanisms mediating the reduction in expression. However, the 50% decrease in gene dosage alone seems insufficient to explain the severe reduction (Figures 4 and 6) and/or transcriptional deficiency observed (see supplemental Figure S9 at *http://ajp.amjpathol.org*) in some of the cell lines and primary lung cancers. A recent study demonstrated a result suggesting the involvement of several transcription factors, such as FKHD, ETS2, INκB, and SOX5, in the regulation of DUSP6 expression.[6] ETS2 is known to be activated via the MEK-ERK cascade,[38,39] and is a pivotal effector inducible of premature senescence as described above.[27–32] On the other hand, FKHD is a downstream target of PI3K, which could be activated indirectly by oncogenic EGFR or KRAS.[2,36] It is speculated that potential alterations of such factors might be an additional mechanism causing the severe reduction and/or transcriptional deficiency of DUSP6 in lung cancers. Further detailed investigation will be required to test this notion.

In summary, the present study has suggested that DUSP6 could be a growth suppressor whose down-regulation is involved in the progression process of lung cancers. We hope our efforts will contribute to a better understanding of carcinogenesis of the lung.

Acknowledgments

We especially thank Masaichi Ikeda (Department of Pathology, Yokohama City University Graduate School of Medicine) and Mamiko Nakamura, Emi Honda, and Sigeko Iwanade (Division of Pathology, Kanagawa Prefectural Cardiovascular Center Hospital) for their excellent technical assistance.

References

1. Kitamura H, Kameda Y, Ito T, Hayashi H: Atypical adenomatous hyperplasia of the lung. Implications for the pathogenesis of peripheral lung adenocarcinoma Am J Clin Pathol 2000, 113:610–620

2. Okudela K, Hayashi H, Ito T, Yazawa T, Suzuki T, Nakane Y, Sato H, Ishi H, KeQin X, Masuda A, Takahashi T, Kitamura H: K-ras gene mutation enhances motility of immortalized airway cells and lung adenocarcinoma cells via Akt activation: possible contribution to non-invasive expansion of lung adenocarcinoma. Am J Pathol 2004, 164:91–100
3. Sharpless NE, DePinho RA: Telomeres, stem cells, senescence, and cancer. J Clin Invest 2004, 113:160–168
4. Sato M, Vaughan MB, Girard L, Peyton M, Lee W, Shames DS, Ramirez RD, Sunaga N, Gazdar AF, Shay JW, Minna JD: Multiple oncogenic changes (K-RAS (V12), p53 knockdown, mutant EGFRs, p16 bypass, telomerase) are not sufficient to confer a full malignant phenotype on human bronchial epithelial cells. Cancer Res 2006, 66:2116–2128
5. Li C, Scott DA, Hatch E, Tian X, Mansour SL: Dusp6 (Mkp3) is a negative feedback regulator of FGF-stimulated ERK signaling during mouse development. Development 2007, 134:167–176
6. Ekerot M, Stavridis MP, Delavaine L, Mitchell MP, Staples C, Owens DM, Keenan ID, Dickinson RJ, Storey KG, Keyse SM: Negative feedback regulation of FGF signalling by DUSP6/MKP-3 is driven by ERK1/2 and mediated by Ets factor binding to a conserved site within the DUSP6/MKP-3gene promoter. Biochem 2008, 412:287–298
7. Muda M, Boschert U, Dickinson R, Martinou JC, Martinou I, Camps M, Schlegel W, Arkinstall S: MKP-3, a novel cytosolic protein-tyrosine phosphatase that exemplifies a new class of mitogen-activated protein kinase phosphatase. J Biol Chem 1996, 271:4319–4326
8. Muda M, Theodosiou A, Rodrigues N, Boschert U, Camps M, Gillieron C, Davies K, Ashworth A, Arkinstall S: The dual specificity phosphatases M3/6 and MKP-3 are highly selective for inactivation of distinct mitogen-activated protein kinases. J Biol Chem 1996, 271:27205–27208
9. Keyse SM: Dual-specificity MAP kinase phosphatases (MKPs) and cancer. Cancer Metastasis Rev 2008, 27:253–261
10. Warmka JK, Mauro LJ, Wattenberg EV: Mitogen-activated protein kinase phosphatase-3 is a tumor promoter target in initiated cells that express oncogenic Ras. J Biol Chem 2004, 279:33085–33092
11. Owens DM, Keyse SM: Differential regulation of MAP kinase signalling by dual-specificity protein phosphatases. Oncogene 2007, 26:3203–3213
12. Furukawa T, Yatsuoka T, Youssef EM, Abe T, Yokoyama T, Fukushige S, Soeda E, Hoshi M, Hayashi Y, Sunamura M, Kobari M, Horii A: Genomic analysis of DUSP6, a dual specificity MAP kinase phosphatase, in pancreatic cancer. Cytogenet Cell Genet 1998, 82:156–159
13. Furukawa T, Sunamura M, Motoi F, Matsuno S, Horii A: Potential tumor suppressive pathway involving DUSP6/MKP-3 in pancreatic cancer. Am J Pathol 2003, 162:1807–1815
14. Furukawa T, Fujisaki R, Yoshida Y, Kanai N, Sunamura M, Abe T, Takeda K, Matsuno S, Horii A: Distinct progression pathways involving the dysfunction of DUSP6/MKP-3 in pancreatic intraepithelial neoplasia and intraductal papillary-mucinous neoplasm's of the pancreas. Mod Pathol 2005, 18:1034–1042
15. Furukawa T: Molecular genetics of intraductal papillary-mucinous neoplasms of the pancreas. J Hepatobiliary Pancreat Surg 2007, 14:233–237
16. Xu S, Furukawa T, Kanai N, Sunamura M, Horii: A Abrogation of DUSP6 by hypermethylation in human pancreatic cancer. J Hum Genet 2005, 50:159–167
17. Chen HY, Yu SL, Chen CH, Chang GC, Chen CY, Yuan A, Cheng CL, Wang CH, Terng HJ, Kao SF, Chan WK, Li HN, Liu CC, Singh S, Chen WJ, Chen JJ, Yang PC: A five-gene signature and clinical outcome in non-small-cell lung cancer. N Engl J Med 2007, 356:11–20
18. Sato H, Yazawa T, Suzuki T, Shimoyamada H, Okudela K, Ikeda M, Hamada K, Yamada-Okabe H, Yao M, Kubota Y, Takahashi T, Kamma H, Kitamura H: Growth regulation via insulin-like growth factor binding protein-4 and -2 in association with mutant K-ras in lung epithelia. Am J Pathol 2006, 169:1550–1566
19. Cozens AL, Yezzi MJ, Kunzelmann K, Ohrui T, Chin L, Eng K, Finkbeiner WE, Widdicombe JH, Gruenert DC: CFTR expression and chloride secretion in polarized immortal human bronchial epithelial cells. Am J Respir Cell Mol Biol 1994, 10:38–47
20. Masuda A, Kondo M, Saito T, Yatabe Y, Kobayashi T, Okamoto M, Suyama M, Takahashi T, Takahashi T: Establishment of human peripheral lung epithelial cell lines (HPL1) retaining differentiated characteristics and responsiveness to epidermal growth factor, hepatocyte growth factor, and transforming growth factor beta1. Cancer Res 1997, 57:4898–4904
21. Ward R, Hawkins N, O'Grady R, Sheehan C, O'Connor T, Impey H, Roberts N, Fuery C, Todd A: Restriction endonuclease-mediated selective polymerase chain reaction: a novel assay for the detection of K-ras mutations in clinical samples. Am J Pathol 1998, 153:373–379
22. Travis WD, Brambilla E, Muller-Hermelink HK, Harris CC (Eds): World Health Organization Classification of Tumors. Pathology and Genetics of the Lung, Pleura, Thymus and Heart. IARC Press: Lyon 2004
23. Bermudez O, Marchetti S, Pagès G, Gimond C: Post-translational regulation of the ERK phosphatase DUSP6/MKP3 by the mTOR pathway. Oncogene 2008, 27:3685–3691
24. Marchetti S, Gimond C, Chambard JC, Touboul T, Roux D, Pouysségur J, Pagès G: Extracellular signal-regulated kinases phosphorylate mitogen-activated protein kinase phosphatase 3/DUSP6 at serines 159 and 197, two sites critical for its proteasomal degradation. Mol Cell Biol 2005, 25:854–864
25. Pierceall WE, Ananthaswamy HN: Transformation of NIH3T3 cells by transfection with UV-irradiated human c-Ha-ras-1 proto-oncogene DNA. Oncogene 1991, 6:2085–2091
26. Takiguchi Y, Takahashi Y, Kuriyama T, Miyamoto T: NIH3T3 transfectant containing human K-ras oncogene shows enhanced metastatic activity after in vivo tumor growth or co-culture with fibroblasts. Clin Exp Metastasis 1992, 10:351–360
27. Ohtani N, Zebedee Z, Huot TJ, Stinson JA, Sugimoto M, Ohashi Y, Sharrocks AD, Peters G, Hara E: Opposing effects of Ets and Id proteins on p16INK4a expression during cellular senescence. Nature 2001, 409:1067–1070
28. Serrano M, Lin AW, McCurrach ME, Beach D, Lowe SW: Oncogenic ras provokes premature cell senescence associated with accumulation of p53 and p16INK4a. Cell 1997, 88:593–602
29. Marcotte R, and E. Wang: Replicative senescence revisited. J Gerontol A Biol Sci Med Sci 2002, 57:B257–B269
30. Sreeramaneni R, Chaudhry A, McMahon M, Sherr CJ, Inoue K: Ras-Raf-Arf signaling critically depends on the Dmp1 transcription factor. Mol Cell Biol 2005, 25:220–232
31. Zhang X, Kim J, Ruthazer R, McDevitt MA, Wazer DE, Paulson KE, Yee AS: The HBP1 transcriptional repressor participates in RAS-induced premature senescence. Mol Cell Biol 2006, 26:8252–8266
32. Huot TJ, Rowe J, Harland M, Drayton S, Brookes S, Gooptu C, Purkis P, Fried M, Bataille V, Hara E, Newton-Bishop J, Peters G: Biallelic mutations in p16 (INK4a) confer resistance to Ras- and Ets-induced senescence in human diploid fibroblasts. Mol Cell Biol 2002, 22:8135–8143
33. Woo T, Okudela K, Yazawa T, Wada N, Ogawa N, Ishiwa N, Tajiri M, Rino Y, Kitamura H, Masuda M: Prognostic value of KRAS mutations and Ki-67 expression in stage I lung adenocarcinomas. Lung Cancer 2009, In Press
34. Shigematsu H, Gazdar AF: Somatic mutations of epidermal growth factor receptor signaling pathway in lung cancers. Int J Cancer 2006, 118:257–262
35. Speake G, Holloway B, Costello G: Recent developments related to the EGFR as a target for cancer chemotherapy. Curr Opin Pharmacol 2005, 5:343–349
36. Feig LA, Schaffhausen B: Signal transduction. The hunt for Ras targets. Nature 1994, 370:527–532
37. Esteller M: Epigenetic gene silencing in cancer: the DNA hypermethylome. Hum Mol Genet 2007, 16:R50–R59
38. Yang SH, Yates PR, Whitmarsh AJ, Davis RJ, Sharrocks AD: The Elk-1 ETS-domain transcription factor contains a mitogen-activated protein kinase targeting motif. Mol Cell Biol 1998, 18:710–720
39. Sharrocks AD: The ET: S-domain transcription factor family. Nat Rev Mol Cell Biol 2001, 2:827–837

MiR-21 is an EGFR-regulated anti-apoptotic factor in lung cancer in never-smokers

Masahiro Seike[a,b], Akiteru Goto[a], Tetsuya Okano[a,b], Elise D. Bowman[a], Aaron J. Schetter[a], Izumi Horikawa[a], Ewy A. Mathe[a], Jin Jen[c], Ping Yang[d], Haruhiko Sugimura[e], Akihiko Gemma[b], Shoji Kudoh[b], Carlo M. Croce[f,1], and Curtis C. Harris[a,1]

[a]Laboratory of Human Carcinogenesis, Center for Cancer Research, National Cancer Institute, National Institutes of Health, Bethesda, MD 20892; [b]Department of Pulmonary Medicine/Infection and Oncology, Nippon Medical School, Tokyo 113-8602, Japan; [c]Division of Pulmonary and Critical Care Medicine and Microarray Share Resources, Mayo Clinic and Foundation, Rochester, MN 55905; [d]Department of Health Sciences Research, Mayo Clinic College of Medicine, Rochester, MN 55905; [e]Department of Pathology, Hamamatsu University School of Medicine, Hamamatsu 431-3192, Japan; and [f]Molecular Virology, Immunology and Medical Genetics, Ohio State University Comprehensive Cancer Center, Columbus, OH 43212

Contributed by Carlo M. Croce, June 1, 2009 (sent for review January 12, 2009)

Fifteen percent of lung cancer cases occur in never-smokers and show characteristics that are molecularly and clinically distinct from those in smokers. Epidermal growth factor receptor (*EGFR*) gene mutations, which are correlated with sensitivity to EGFR-tyrosine kinase inhibitors (EGFR-TKIs), are more frequent in never-smoker lung cancers. In this study, microRNA (miRNA) expression profiling of 28 cases of never-smoker lung cancer identified aberrantly expressed miRNAs, which were much fewer than in lung cancers of smokers and included miRNAs previously identified (e.g., up-regulated miR-21) and unidentified (e.g., down-regulated miR-138) in those smoker cases. The changes in expression of some of these miRNAs, including miR-21, were more remarkable in cases with *EGFR* mutations than in those without these mutations. A significant correlation between phosphorylated-EGFR (*p*-EGFR) and miR-21 levels in lung carcinoma cell lines and the suppression of miR-21 by an EGFR-TKI, AG1478, suggest that the EGFR signaling is a pathway positively regulating miR-21 expression. In the never-smoker–derived lung adenocarcinoma cell line H3255 with mutant *EGFR* and high levels of *p*-EGFR and miR-21, antisense inhibition of miR-21 enhanced AG1478-induced apoptosis. In a never-smoker–derived adenocarcinoma cell line H441 with wild-type *EGFR*, the antisense miR-21 not only showed the additive effect with AG1478 but also induced apoptosis by itself. These results suggest that aberrantly increased expression of miR-21, which is enhanced further by the activated EGFR signaling pathway, plays a significant role in lung carcinogenesis in never-smokers, as well as in smokers, and is a potential therapeutic target in both *EGFR*-mutant and wild-type cases.

apoptosis | microRNA | microarray | EGFR-TKI | therapeutic target

Approximately 10% to 25% of all lung cancer cases are not attributable to smoking (1, 2). Recent studies that pay specific attention to lung cancers in never-smokers have suggested that these cancers have characteristics distinct from those in smokers (2): G-to-T transversions of the *p53* and *K-ras* mutations occur less frequently in lung adenocarcinomas from never-smokers than in those from smokers (3–6), and mutations of epidermal growth factor receptor (*EGFR*) gene are observed more frequently in never-smoker cases (6). A profiling of global gene expression in never-smoker lung cancers may provide novel molecular and clinical aspects in lung carcinogenesis. Although EGFR tyrosine kinase inhibitors (EGFR-TKIs), including gefitinib and erlotinib, currently are in clinical use and are preferentially effective in *EGFR*-mutant cases (7, 8), as many as 30% of *EGFR*-mutant cases and 90% of *EGFR* wild-type cases showed no therapeutic response to EGFR-TKIs (9). Therefore, identification of a new therapeutic target and development of a method to improve the EGFR-TKI therapy will be of critical importance for the better treatment of lung cancer.

MicroRNAs (miRNAs) are small, non-coding RNA molecules of about 18 to 25 nucleotides that frequently are located at chromosomal regions deleted or amplified in cancers, suggesting that miRNAs are a class of genes involved in human tumorigenesis (10). Expression levels of miRNAs are altered in various types of human cancers, including lung cancers (11–18). Recently, miRNAs have been demonstrated to be diagnostic and prognostic markers in leukemia, lung cancer, and colon cancer (13, 18–19). It also is suggested that miRNAs can be a therapeutic target in human cancers (20). We previously analyzed miRNA expression profiles of 104 lung cancers, 99 of which were from smokers, and found that high expression of miR-155, miR-21, and miR-106a, as well as low expression of let-7a, correlated with poor survival (18). In the present study we investigate a global expression profile of miRNAs in lung cancers from never-smokers. Comparisons of miRNA expression in never-smoker versus smoker cases and in *EGFR* wild-type versus mutant cases find different profiles of miRNA expression associated with smoking status and reveal EGFR-mediated regulation of miRNA expression. Our in vitro functional analyses also suggest that the inhibition of miR-21, whose up-regulation is associated with *EGFR* mutations, can be a potential therapeutic strategy in combination with EGFR-TKI treatment or by itself.

Results

MicroRNA Expression Profiles in Lung Cancers from Never-Smokers. We examined miRNA expression profiles in 28 matched pairs of lung cancer and noncancerous lung tissues from never-smokers (Table 1 and supporting information (SI) Table S1) using the Ohio State miRNA microarray version 3.0 (21). In class comparison analysis using National Cancer Institute Division of Treatment and Diagnosis Biometric Research Branch (BRB) array tools, 18 miRNAs were found to be differentially expressed in cancers compared with noncancerous tissues [$P < 0.01$ with a false-discovery rate (FDR) of < 0.15)] (Table 2). The expression profiles of these 18 miRNAs distinguished cancer and paired noncancerous tissues with a prediction accuracy of 84% using the 3-nearest-neighbor algorithm and an accuracy of 82% using the support vector machine algorithm within BRB array tools (10-fold cross validation repeated 100 times). Expression levels of 5 miRNAs were higher in cancer tissues, with miR-21 enriched the most, at 2.35-fold. Expression levels of 13 miRNAs were lower in cancers, with miR-486 and miR-126* repressed the most, at 0.45-fold. The validity of the analysis was supported by the identification of a single miRNA by

Author contributions: M.S., A. Goto, I.H., E.A.M., A. Gemma, C.M.C., and C.C.H. designed research; M.S., A. Goto, T.O., E.D.B., A.J.S., I.H., and C.C.H. performed research; E.D.B., J.J., P.Y., H.S., S.K., and C.M.C. contributed new reagents/analytic tools; M.S., A. Goto, A.J.S., I.H., E.A.M., C.M.C., and C.C.H. analyzed data; and M.S., I.H., C.M.C., and C.C.H. wrote the paper.

The authors declare no conflict of interest.

Data deposition: The microRNA microarray data have been deposited in the Gene Expression Omnibus (GEO) (http://www.ncbi.nlm.nih.gov/geo/, GSE14936).

[1]To whom correspondence may be addressed. E-mail: Curtis_Harris@nih.gov or carlo.croce@osumc.edu.

This article contains supporting information online at www.pnas.org/cgi/content/full/0905234106/DCSupplemental.

Table 1. Characteristics of never-smoker patients with non-small cell lung cancer

Characteristic	No. of patients
Histology	
Adenocarcinoma	22 (78%)
Squamous cell carcinoma	4 (14%)
Adenosquamous cell carcinoma	1 (4%)
Unclassified	1 (4%)
Stage	
I	21 (75%)
II–IV	7 (25%)
Age	
≤ 65	18 (64%)
> 65	10 (36%)
Gender	
Female	18 (64%)
Male	10 (36%)
Race	
Caucasian	19 (68%)
African American	3 (11%)
Asian (Japanese)	6 (21%)
EGFR gene status	
Wild-type	22 (79%)
Mutant	6 (21%)

2 different probes (miR-21, miR-521, and miR-516a), of 2 mature miRNAs generated from a single stem-loop pre-miRNA (miR-126 and miR-126*), and of more than 1 miRNA chromosomally clustered and possibly co-regulated (miR-30a and miR-30c on 6q13; miR-30b and miR-30d on 8q24.22; and miR-516a, miR-520, and miR-521 on 19q13.41)]. The mRNA microarray data of never-smoker lung adenocarcinoma cases (22) (http://www.ncbi.nlm.nih.gov/geo/, accession number = GSE10072) also showed that 2 host genes, *TMEM49* and *EGFL7* (Table 2), were differentially expressed in cancer and noncancerous tissues in the same directions as their resident miRNAs (miR-21 and miR-126/126*, respectively). The expression levels of 3 miRNAs (miR-21, miR-126, and miR-486) were examined by real-time quantitative RT-PCR (qRT-PCR) (Fig. S1). MiR-21 expression was significantly higher in cancer tissues than in noncancerous tissues ($P < 0.05$, paired t-test) (Fig. S1*A*), and miR-126 and miR-486 were expressed at significantly lower levels in cancers (each $P < 0.05$, paired t-test) (Fig. S1 *B* and C), further validating the results of the microarray analysis.

Differential miRNA Profiles in Lung Cancers from Never-Smokers Versus Smokers. To identify cancer-associated changes in miRNA expression that are related to smoking status, we compared the miRNA expression profiles of the present never-smoker cases with those of 58 smoker lung adenocarcinoma cases in our previous study (18) and 23 additional cases of lung adenocarcinoma in smokers (Table S2). We identified 5 miRNAs that commonly were changed in expression in never-smoker and smoker cases, among which was the increased miR-21 (Table S3). Although only 2 miRNAs, miR-138 and let-7c, were changed significantly (both were down-regulated) in never-smoker cases, the altered expression of 36 miRNAs was preferentially associated with smoker cases (Table S3), probably reflecting the more extensive genetic and epigenetic changes in smoker-derived lung cancers (23). By qRT-PCR we validated the specific down-regulation of miR-138 in never-smoker adenocarcinomas and the up-regulation of miR-21 and the down-regulation of miR-126* irrespective of smoking status (Fig. S2). Interestingly, miR-138 is located at chromosome 3p21.33, a candidate locus that carries a lung cancer suppressor gene (24), and was reported to target the human telomerase reverse transcriptase gene (*hTERT*) (25) on which a variety of cellular and viral oncogenic mechanisms act (26). A role for this miRNA in the etiology of lung cancers from never-smokers deserves further investigation.

MiRNA Expression Profiles Associated with *EGFR* Gene Mutations. The status of the *EGFR* gene was determined by DNA sequencing in the

Table 2. miRNAs differentially expressed in lung cancer tissues and normal lung tissues from 28 never-smokers

Mature miR	Probe	Location	P-value†	FDR‡	Type§	Ratio¶	Host gene‖
miR-21	hsa-mir-21-prec-17	17q23.1	3.0E-04	0.01	Up	2.35	*TMEM49*
miR-21	hsa-mir-21–1	17q23.1	9.6E-04	0.03	Up	2.22	*TMEM49*
miR-141	hsa-mir-141-prec-1	12p13.31	0.001	0.03	Up	1.50	Intergenic
miR-210	hsa-mir-210-prec	11p15.5	0.002	0.06	Up	1.51	Intergenic
miR-200b	hsa-mir-200b	1p36.33	0.008	0.11	Up	1.39	Intergenic
miR-346	hsa-mir-346	10q23.2	0.009	0.12	Up	1.14	*GRID-1*
miR-126*	hsa-mir-126*-1	9q34.3	3.5E-05	0.01	Down	0.45	*EGFL7*
miR-126	hsa-mir-126	9q34.3	0.004	0.07	Down	0.69	*EGFL7*
miR-30a	hsa-mir-30a-prec-1	6q13	1.4E-04	0.01	Down	0.61	*C6orf155*
miR-30d	hsa-mir-30d-prec-2	8q24.22	1.5E-04	0.01	Down	0.57	Intergenic
miR-486	hsa-mir-486	8p11.21	2.7E-04	0.01	Down	0.45	Intergenic
miR-129	hsa-mir-129–2	11p11.2	2.8E-04	0.01	Down	0.77	Intergenic
miR-451	hsa-mir-451–1	17q11.2	4.8E-04	0.02	Down	0.46	Intergenic
miR-521	hsa-mir-521–2	19q13.41	0.005	0.08	Down	0.84	Intergenic
miR-521	hsa-mir-521–1	19q13.41	0.005	0.08	Down	0.80	Intergenic
miR-138	hsa-mir-138–1-prec	3p21.33	0.006	0.10	Down	0.72	Intergenic
miR-30b	hsa-mir-30b-prec	8q24.22	0.006	0.10	Down	0.58	Intergenic
miR-30c	hsa-mir-30c-prec	6q13	0.007	0.11	Down	0.61	*C6orf155*
miR-516a	hsa-mir-516a-1	19q13.41	0.008	0.11	Down	0.89	Intergenic
miR-516a	hsa-mir-516a-2	19q13.41	0.010	0.12	Down	0.90	Intergenic
miR-520	hsa-mir-520 h	19q13.41	0.009	0.12	Down	0.84	Intergenic

†miRNA-microarray analysis was performed using pairs of tumors and corresponding normal tissues from 28 never-smokers ($P < 0.01$).
‡False-discovery rate (FDR) < 0.15.
§Up, up-regulated in tumors compared with normal tissue; down, down-regulated in tumors compared with normal tissue.
¶Ratio of tumor to normal tissue.
‖http://microrna.sanger.ac.uk/sequences/.

Table 3. miRNAs differentially expressed in *EGF*-mutant and wild-type lung cancers from never-smokers

Mature miR	Probe	Location	P-value†	FDR†	Type§	Ratio¶
miR-21	hsa-mir-21–1	17q23.1	0.001	0.05	Up	1.79
	hsa-mir-21-prec-17	17q23.1	0.001	0.04	Up	1.67
miR-210	hsa-mir-210-prec	11p15.5	0.007	0.13	Up	1.20
miR-129	hsa-mir-129–2	11p11.2	0.001	0.05	Up	1.06
miR-486	hsa-mir-486	8p11.21	0.001	0.04	Down	0.60
miR-126	hsa-mir-126–2	9q34.3	0.003	0.08	Down	0.69
miR-126*	hsa-mir-126*-1	9q34.3	0.0005	0.04	Down	0.70
miR-138	hsa-mir-138–1-prec	3p21.33	0.004	0.10	Down	0.69
miR-521	hsa-mir-521–1	19q13.41	0.005	0.11	Down	0.81
	hsa-mir-521–2	19q13.41	0.003	0.08	Down	0.82
miR-451	hsa-mir-451–1	17q11.2	0.002	0.07	Down	0.81
miR-141	hsa-mir-141-prec-1	12p13.31	0.004	0.10	Down	0.85
miR-30d	hsa-mir-30d-prec-2	8q24.22	0.001	0.04	Down	0.93
miR-30a	hsa-mir-30a-prec-1	6q13	0.001	0.04	Down	0.95

†Class comparison analysis was performed between 22 *EGFR* wild-type and 6 mutant tumors ($P < 0.01$).
‡False-discovery rate (FDR) < 0.15.
§Up, up-regulated in *EGFR*-mutant compared with wild-type tumors; down, down-regulated in *EGFR*-mutant compared with wild-type tumors.
¶Ratio of tumors with mutant *EGFR* to tumors with wild-type *EGFR*.

28 lung cancer tissues from never-smokers, and 6 cases were found to have the activating mutations of *EGFR* in the tyrosine kinase domain (Table S1). The class comparison analysis of miRNA expression between 22 *EGFR* wild-type and 6 *EGFR*-mutant cases found 12 miRNAs that were significantly more or less abundant in *EGFR*-mutant cases ($P < 0.01$ with FDR < 0.15) (Table 3). Of the 12 miRNAs, 10 (miR-21, miR-210, miR-486, miR-126, miR-126*, miR-138, miR-521, miR-451, miR-30d, and miR-30a) were changed in the same direction as in cancer versus noncancerous tissues (Table 2), suggesting that *EGFR* mutations may reinforce the aberrant regulation of some miRNAs associated with lung carcinogenesis in never-smokers. MiR-21 and miR-486, which were most up-regulated and most down-regulated, respectively, in cancerous versus noncancerous tissues, again showed the greatest difference between *EGFR*-mutant and wild-type cancers (≈1.7-fold and 0.60-fold, respectively). Although the qRT-PCR data shown in Fig. S1 reflect a limited number of cases, limiting our ability to show a statistically significant difference between *EGFR*-mutant and wild-type cases in the expression of miR-21, miR-126, or miR-486, the 3 cases expressing the highest levels of miR-21 in cancer (cases 24, 25, and 28) had the activating mutation of *EGFR* (Fig. S1*A* and Table S1).

Expression of miR-21 and the Status of EGFR Signaling in Lung Cancer Cell Lines. Because of its most remarkable increase in cancer as compared with noncancerous tissues and its association with *EGFR* mutations, an indicator of sensitivity to EGFR-TKIs (9), miR-21 was chosen for further analyses. To investigate a correlation between miR-21 expression levels and the status of EGFR signaling pathway, 8 non-small cell lung cancer (NSCLC) cell lines were examined in Western blot (Fig. S3 *A*, *B*, and *C*) and qRT-PCR analyses (Fig. 1*A*). Among them, 3 adenocarcinoma cell lines (H3255, H1975, and H1650) were mutant for *EGFR*, as reported (8, 27–29). These 3 *EGFR*-mutant cell lines had high levels of phosphorylated EGFR (*p*-EGFR), as well as increased amounts of total EGFR protein and induction of phosphorylated Akt (*p*-Akt) (Fig. S3*C*), consistent with the constitutive activation of the EGFR signaling pathway in these cells (28, 29). Of the 3 cell lines, H3255 and H1975, but not H1650, expressed elevated levels of miR-21 (Fig. 1*A*). Of 5 *EGFR* wild-type cell lines, 3, either with (H441) or without (A549 and H1299) detectable levels of *p*-EGFR (Fig. S3 *A* and *B*), also expressed significantly higher levels of miR-21 than seen in control untransformed cells (Fig. 1*A*). The quantitative comparison of miR-21 and *p*-EGFR levels showed a significant positive correlation between these 2 factors (Pearson's correlation,

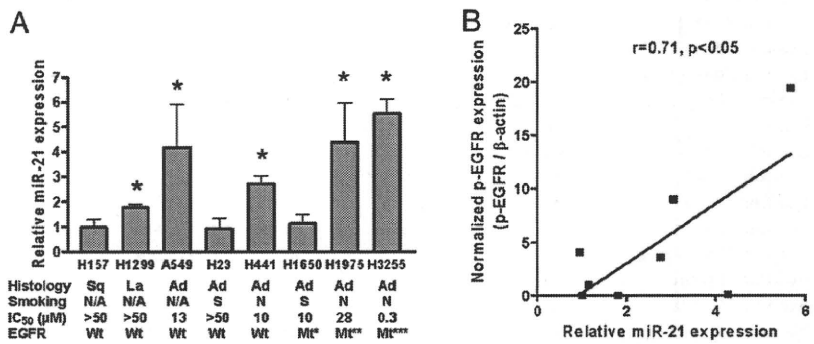

Fig. 1. MiR-21 expression in human lung cancer cell lines. (*A*) MiR-21 expression levels were analyzed by qRT-PCR and expressed relative to *hTERT*-immortalized normal human bronchial epithelial cells (HBET2) (defined as 1.0, not shown). Data were mean ± SD from 3 independent experiments. The suppressive effects of AG1478 on cell growth were determined by MTS assay and indicated as IC_{50}. *, $P < 0.05$ when compared with HBET2, Student's *t*-test. Ad, adenocarcinoma; La, large cell carcinoma; Mt*, *EGFR* mutant ΔE746-A750 (in-frame deletion of codons 746 to 750); Mt**, L858R (substitution from leucine to arginine at codon 858) and T790M (substitution from threonine to methionine at codon 790); Mt***, L858R; N/A, information not available; N, derived from never-smoker cases; S, derived from smoker cases; Sq, squamous cell carcinoma; Wt, *EGFR* wild-type. (*B*) Correlation between miR-21 expression and *p*-EGFR levels (Pearson's correlation, $r = 0.71$, $P < 0.05$). The miR-21 data were from panel *A*, and the *p*-EGFR data were obtained by quantitatively analyzing the results shown in Fig. S3.

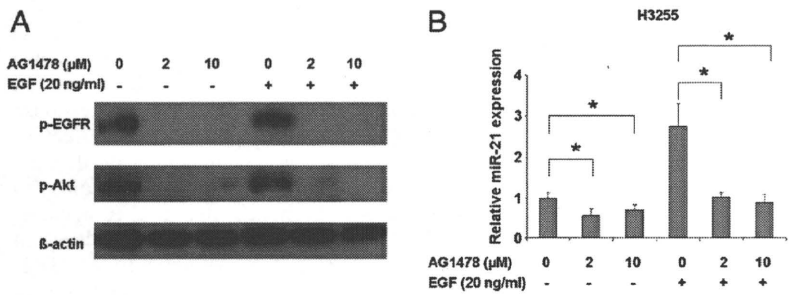

Fig. 2. AG1478 represses miR-21 expression. H3255 lung adenocarcinoma cells, characterized by a high expression of miR-21 and *EGFR* mutation, were serum starved for 24 h and then were grown in either the presence or absence of AG1478 (2 μM or 10 μM) for 2 h with or without following exposure to 20 ng/mL EGF for 15 min. (*A*) The effect of AG1478 on *p*-EGFR and *p*-Akt expression. β-actin was a loading control. (*B*) MiR-21 expression levels analyzed by qRT-PCR after the AG1478 treatments (2 μM or 10 μM) with or without EGF ligand stimulation. MiR-21 expression levels were expressed as values relative to untreated cells in the absence of EGF. Data were mean ± SD from 4 independent experiments. *, $P < 0.05$, paired *t*-test.

$r = 0.71, P < 0.05$) (Fig. 1*B*). These results suggest that the activated EGFR signaling pathway can be functionally associated with miR-21 up-regulation. It also was noteworthy that miR-21 expression and/or *EGFR* status correlated with sensitivity (indicated as IC_{50}) to an EGFR-TKI, AG1478 (Fig. 1*A*); the 5 cell lines showing AG1478-inhibited cell proliferation either had mutant *EGFR* (H1650) or expressed > 2-fold increased levels of miR-21 (H441 and A549), or both (H3255 and H1975). We selected 2 lung adenocarcinoma cell lines derived from never-smoker cancers for the functional assays of miR-21: H3255 with high sensitivity to AG1478 (IC_{50}, 0.3 μM), mimicking never-smoker lung cancer cases with mutant *EGFR* and the highest levels of miR-21 (e.g., case numbers 24, 25, and 28 in Fig. S1*A* and Table S1); and H441 with intermediate sensitivity to AG1478 (IC_{50}, 10 μM), mimicking never-smoker lung cancer cases with wild-type *EGFR* but with significantly increased levels of miR-21 (e.g., case numbers 5 and 23 in Fig. S1*A* and Table S1).

Activated EGFR Signaling Enhances miR-21 Expression. *EGFR*-mutant H3255 cells were treated with AG1478 in the presence or absence of EGF (Fig. 2). AG1478 at either 2 μM or 10 μM effectively inhibited the EGFR signaling under conditions with or without EGF ligand stimulation, as shown by diminished *p*-EGFR and *p*-Akt (Fig. 2*A*), consistent with the IC_{50} value of 0.3 μM in this cell line. The levels of miR-21 expression in the absence of EGF were significantly repressed by treatment with either concentration of AG1478 ($P < 0.01$, paired *t*-test) (Fig. 2*B*, *Left*). The addition of EGF resulted in ≈2.5-fold up-regulation of miR-21 expression, which still was inhibited back to the basal levels by treatment with either concentration of AG1478 ($P < 0.05$, paired *t*-test) (Fig. 2*B*, *Right*). These results indicate that miR-21 expression is positively regulated by the activated EGFR signaling in cancer cells with an activating *EGFR* mutation and that EGFR-TKIs can effectively repress the aberrantly increased miR-21. In H441 cells with wild-type *EGFR*, AG1478 at 10 μM (equivalent to the IC_{50} value in this cell line), but not at 2 μM, significantly repressed miR-21 expression ($P < 0.05$, paired *t*-test) (Fig. S4). Thus, the activated signaling from wild-type EGFR in H441 cells (Fig. S3*B*), probably through a self-produced TGF-alpha stimulation (28), also can be inhibited by AG1478, resulting in the repression of miR-21.

Antisense Inhibition of miR-21 Induces Apoptosis in Cooperation with EGFR-TKI. H3255 and H441 cells were transfected with an antisense oligonucleotide targeting miR-21 (anti-miR-21). The antisense-mediated repression of miR-21 in these cells was confirmed by qRT-PCR (Fig. 3*A*). Because miR-21 reportedly has an anti-apoptotic activity (30), we used an assay measuring caspase-3 and caspase-7 enzymatic activities to determine whether inhibition of miR-21 induces apoptosis in these cells (Fig. 3 *B* and *C*). In H3255 cells, anti-miR-21 alone did not induce apoptosis (Fig. 3*B*, *Left*). Notably, however, when used in combination with AG1478 at 0.2 μM (a concentration slightly lower than the IC_{50} value), anti-miR-21 significantly enhanced AG1478-induced apoptotic response (Fig. 3*B*, *Right*). In H441 cells, anti-miR-21 by itself resulted in a significant increase in apoptotic response (Fig. 3*C*, *Left*), although it was less effective than AG1478 treatment at 10 μM (a concentration equivalent to the IC_{50} value). Similar to the combinational effect observed in H3255 cells, anti-miR-21 further enhanced apoptotic response induced by 10 μM of AG1478 in H441 cells (Fig. 3*C*, *Right*). The effect of anti-miR-21 on apoptosis was substantiated further by Western blot analysis of poly (ADP-ribose) polymerase (PARP), a main cleavage target of caspase-3 in the apoptotic response (Fig. 3*D*). The amounts of uncleaved PARP were markedly decreased in H3255 cells treated with both anti-miR-21 and AG1478 and in H441 cells treated with anti-miR-21 in the presence or absence of AG1478, where anti-miR-21 caused significant increases in caspase 3/7 activities.

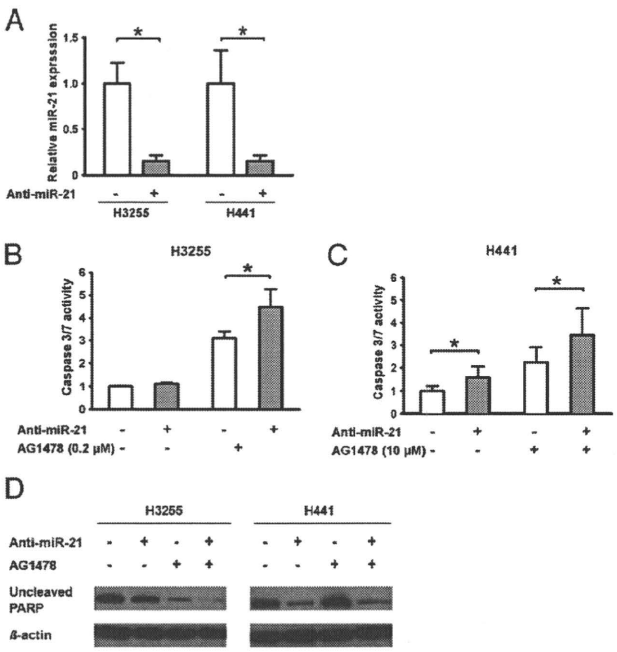

Fig. 3. Inhibition of miR-21 enhances AG1478-induced apoptosis. (*A*) Cells were transfected with 40 nM of anti-miR-21 (+) or control oligonucleotide (anti-EGFP) (−) for 72 h and examined by qRT-PCR. The expression levels of miR-21 after transfection of anti-miR-21 were expressed as the relative values to control. Data were mean ± SD from 3 independent experiments. *, $P < 0.05$, paired *t*-test. (*B*, *C*) Cells (H3255 or H441) were transfected with 40 nM of anti-miR-21 (+) or anti-EGFP (−) for 72 h and then were grown in the presence or absence of 0.2 μM of AG1478 for 24 h (H3255) or 10 μM for 72 h (H441). The activities of caspase 3/7 were expressed as the values relative to the activities of cells without anti-miR-21 and AG1478. Data were mean ± SD from at least 4 independent experiments. *, $P < 0.05$, Student's *t*-test. (*D*) Uncleaved PARP was evaluated by Western blot analysis. Cells were transfected with anti-miR-21 or anti-EGFP as described previously and then were grown in the presence or absence of 2 μM of AG1478 for 72 h. β-actin was a loading control.